BIOMETRIC IDENTIFICATION BASED ON EYE MOVEMENTS AND IRIS FEATURES USING TASK-DRIVEN AND TASK-INDEPENDENT STIMULI

by

Ali Alhaj Darwish

A Thesis Presented to the Faculty of the
American University of Sharjah
College of Engineering
in Partial Fulfillment
of the Requirements
for the Degree of

Master of Science in
Computer Engineering

Sharjah, United Arab Emirates

June 2013

Approval Signatures

We, the undersigned, approve the Master's Thesis of Ali Alhaj Darwish

Thesis Title: Biometric Identification Based on Eye Movements and Iris Features Using Task-Driven and Task-Independent Stimuli.

Signature	**Date of Signature** (dd/mm/yyyy)
_____	_____
Dr. Michel Pasquier Associate Professor, Department of Computer Science and Engineering Thesis Advisor	
_____	_____
Dr. Ghassan Zaki Qadah Associate Professor, Department of Computer Science and Engineering Thesis Committee Member	
_____	_____
Dr. Fadi Aloul Associate Professor, Department of Computer Science and Engineering Thesis Committee Member	
_____	_____
Dr. Andrew Marrington Assistant Professor, College of Technological Innovation- Zayed University Thesis Committee Member	
_____	_____
Dr. Assim Sagahyroon Head, Department of Computer Science and Engineering	
_____	_____
Dr. Hany El-Kadi Associate Dean , College of Engineering	
_____	_____
Dr. Leland Blank Interim Dean ,College of Engineering	
_____	_____
Dr. Khaled Assaleh Director of Graduate Studies	

Acknowledgement

I would like to thank my Advisor Dr. Michel Pasquier for the help, support, and advice that he offered me throughout my thesis work.

Further, I would like to thank Dr. Leon Jololian, Dean of the College of Technological Innovation at Zayed University, for giving me the opportunity to conduct the experiments in the university's HCI laboratory.

My beloved country Syria, I dedicate this work to you.

Abstract

This work investigates the feasibility of using the dynamic features of the eyes for biometric identification. Identifying individuals using eye movements is typically limited by a low accuracy, thus preventing this technique from becoming commercially viable. In addition, the human eyes constitute a rich source of information, still only partially understood so far, hence more research is needed to understand exactly what kind of information they can provide, and what technique should be applied to analyze such information. It is also largely unknown what kind of feature will yield accurate data most useful to biometric identification, or which stimuli most influence most the dynamic features of the eyes and their usability as a biometrical trait. We show that, by combining eye movement features and iris constriction and dilation parameters, the dynamic features of the eye can yield a good level of accuracy for biometric systems. The approach consists of recording and categorizing eye movements as well as changes in pupil size into segments consisting of saccades and fixations, and computing for each the many velocity and acceleration features that are used to train the classifier to perform the biometric identification. We tested four types of stimuli to hypothesize which will provide a viable stimulating method for extracting eye features. The results suggest that simple stimuli such as images and graphs can appropriately excite the dynamic features of the eye for the purpose of biometric identification.

Search Terms: *Behavioral Biometrics, Eye-Movement Biometrics, Iris Biometrics, Non-Intrusive Identification, Task-Independent Identification, Stealth Identification, Machine Learning.*

Table of Contents

List of Figures

List of Tables

Nomenclature

mean of eye fixation angular velocity	θ_F^{μ}
standard deviation of fixation angular velocity	θ_F^{σ}
mean of eye movement fixation velocity of the left eye	$\mathcal{V}_{F,L}^{\mu}$
standard deviation of eye movement fixation velocity of the left eye	$\mathcal{V}_{F,L}^{\sigma}$
mean of eye movement fixation acceleration of the left eye	$\varphi_{F,L}^{\mu}$
standard deviation of eye movement fixation acceleration of the left eye	$\varphi_{F,L}^{\sigma}$
mean of eye movement fixation velocity of the right eye	$\mathcal{V}_{F,R}^{\mu}$
standard deviation of eye movement fixation velocity of the right eye	$\mathcal{V}_{F,R}^{\sigma}$
mean of eye movement fixation acceleration of the right eye	$\varphi_{F,R}^{\mu}$
standard deviation of eye movement fixation acceleration of the right eye	$\varphi_{F,R}^{\sigma}$
peak of eye movement fixation velocity of the left eye	$\mathcal{V}_{F,L}^{\rho}$
peak of eye movement fixation acceleration of the left eye	$\varphi_{F,L}^{\rho}$
peak of eye movement fixation velocity of the right eye	$\mathcal{V}_{F,R}^{\rho}$
peak of eye movement fixation acceleration of the right eye	$\varphi_{F,R}^{\rho}$
difference mean of eye movement fixation velocity between left and right eye	$\mathcal{V}_{F,\Gamma}^{\mu}$
difference standard deviation of eye movement fixation velocity between left and right eye	$\mathcal{V}_{F,\Gamma}^{\sigma}$
difference mean of eye movement fixation acceleration between left and right eye	$\varphi_{F,\Gamma}^{\mu}$
standard deviation of eye movement fixation acceleration of the right eye	$\varphi_{F,\Gamma}^{\sigma}$
mean of eye saccade angular velocity	θ_S^{μ}
standard deviation of saccade angular velocity	$\theta_{S_J}^{\sigma}$
mean of eye movement saccade velocity of the left eye	$\mathcal{V}_{S,L}^{\mu}$
standard deviation of eye movement saccade velocity of the left eye	$\mathcal{V}_{S,L}^{\sigma}$

mean of eye movement saccade acceleration of the left eye	$\varphi_{S,L}^{\mu}$
standard deviation of eye movement saccade acceleration of the left eye	$\varphi_{S,L}^{\sigma}$
mean of eye movement saccade velocity of the right eye	$\mathcal{V}_{S,R}^{\mu}$
standard deviation of eye movement saccade velocity of the right eye	$\mathcal{V}_{S,R}^{\sigma}$
mean of eye movement saccade acceleration of the right eye	$\varphi_{S,R}^{\mu}$
standard deviation of eye movement saccade acceleration of the right eye	$\varphi_{S,R}^{\sigma}$
peak of eye movement saccade velocity of the left eye	$\mathcal{V}_{S,L}^{\rho}$
peak of eye movement saccade acceleration of the left eye	$\varphi_{S,L}^{\rho}$
peak of eye movement saccade velocity of the right eye	$\mathcal{V}_{S,R}^{\rho}$
peak of eye movement saccade acceleration of the right eye	$\varphi_{S,R}^{\rho}$
difference mean of eye movement saccade velocity between left and right eye	$\mathcal{V}_{S,\Gamma}^{\mu}$
difference standard deviation of eye movement saccade velocity between left and right eye	$\mathcal{V}_{S,\Gamma}^{\sigma}$
difference mean of eye movement saccade acceleration between left and right eye	$\varphi_{S,\Gamma}^{\mu}$
standard deviation of eye movement saccade acceleration of the right eye	$\varphi_{S,\Gamma}^{\sigma}$
mean of pupil size fixation of the left eye	$\delta_{F,L}^{\mu}$
standard deviation of pupil size fixation of the left eye	$\delta_{F,L}^{\sigma}$
mean of pupil size fixation of the right eye	$\delta_{F,R}^{\mu}$
standard deviation of pupil size fixation of the right eye	$\delta_{F,R}^{\sigma}$
mean of pupil size velocity fixation of the left eye	$\vartheta_{F,L}^{\mu}$
standard deviation of pupil size velocity fixation of the left eye	$\vartheta_{F,L}^{\sigma}$
mean of pupil size acceleration fixation of the left eye	$\alpha_{F,L}^{\mu}$
standard deviation of pupil size acceleration fixation of the left eye	$\alpha_{F,L}^{\sigma}$
peak of pupil size velocity fixation of the left eye	$\vartheta_{F,L}^{\rho}$
peak of pupil size acceleration fixation of the left eye	$\alpha_{F,L}^{\rho}$
mean of pupil size velocity fixation of the right eye	$\vartheta_{F,R}^{\mu}$

standard deviation of pupil size velocity fixation of the left eye	$\vartheta_{F,R}^{\sigma}$
mean of pupil size acceleration fixation of the right eye	$\alpha_{F,R}^{\mu}$
standard deviation of pupil size acceleration fixation of the right eye	$\alpha_{F,R}^{\sigma}$
peak of pupil size velocity fixation of the right eye	$\vartheta_{F,R}^{\rho}$
peak of pupil size acceleration fixation of the right eye	$\alpha_{F,R}^{\rho}$
difference of mean of pupil size velocity fixation between the eyes	$\vartheta_{F,\Gamma}^{\mu}$
difference of standard deviation of pupil size velocity fixation between the eyes	$\vartheta_{F,\Gamma}^{\sigma}$
difference of mean of pupil size acceleration fixation between the eyes	$\alpha_{F,\Gamma}^{\mu}$
difference of standard deviation of pupil size acceleration fixation between the eyes	$\alpha_{F,\Gamma}^{\sigma}$
difference of mean of pupil size fixation between eyes	$\delta_{F,\Gamma}^{\mu}$
difference of standard deviation of pupil size fixation between the eyes	$\delta_{F,\Gamma}^{\sigma}$
difference of peak of pupil size velocity fixation between the eyes	$\vartheta_{F,\Gamma}^{\rho}$
difference of peak of pupil size acceleration fixation between the eyes	$\alpha_{F,\Gamma}^{\rho}$
mean of pupil size saccade of the left eye	$\delta_{S,L}^{\mu}$
standard deviation of pupil size saccade of the left eye	$\delta_{S,L}^{\sigma}$
mean of pupil size saccade of the right eye	$\delta_{S,R}^{\mu}$
standard deviation of pupil size saccade of the right eye	$\delta_{S,R}^{\sigma}$
mean of pupil size velocity saccade of the left eye	$\vartheta_{S,L}^{\mu}$
standard deviation of pupil size velocity saccade of the left eye	$\vartheta_{S,L}^{\sigma}$
mean of pupil size acceleration saccade of the left eye	$\alpha_{S,L}^{\mu}$
standard deviation of pupil size acceleration saccade of the left eye	$\alpha_{S,L}^{\sigma}$
peak of pupil size velocity saccade of the left eye	$\vartheta_{S,L}^{\rho}$
peak of pupil size acceleration saccade of the left eye	$\alpha_{S,L}^{\rho}$
mean of pupil size velocity saccade of the right eye	$\vartheta_{S,R}^{\mu}$

standard deviation of pupil size velocity saccade of the left eye	$\vartheta_{S,R}^{\sigma}$
mean of pupil size acceleration saccade of the right eye	$\alpha_{S,R}^{\mu}$
standard deviation of pupil size acceleration saccade of the right eye	$\alpha_{S,R}^{\sigma}$
peak of pupil size velocity saccade of the right eye	$\vartheta_{S,R}^{\rho}$
peak of pupil size acceleration saccade of the right eye	$\alpha_{S,R}^{\rho}$
difference of mean of pupil size velocity saccade between the eyes	$\vartheta_{S,\Gamma}^{\mu}$
difference of standard deviation of pupil size velocity saccade between the eyes	$\vartheta_{S,\Gamma}^{\sigma}$
difference of mean of pupil size acceleration saccade between the eyes	$\alpha_{S,\Gamma}^{\mu}$
difference of standard deviation of pupil size acceleration saccade between the eyes	$\alpha_{S,\Gamma}^{\sigma}$
difference of mean of pupil size saccade between eyes	$\delta_{S,\Gamma}^{\mu}$
difference of standard deviation of pupil size saccade between the eyes	$\delta_{S,\Gamma}^{\sigma}$
difference of peak of pupil size velocity saccade between the eyes	$\alpha_{S,\Gamma}^{\sigma}$
difference of peak of pupil size acceleration saccade between the eyes	$\alpha_{S,\Gamma}^{\rho}$
distance between the gazes during saccades	D_S
distance between the gazes during fixations	D_F

1 Introduction

Security and data protection are increasingly becoming a major concern due to the huge demand for services provided by access-based systems. Biometric identification seems to fulfill this demand by providing secure, low cost, and convenient access techniques by relying on the anatomy of the human body (e.g., fingerprints [1], facial features [2], and iris matching [3]).

However, counterfeiting and replication of biometrics have become possible with new advances in technology. For example, hackers have discovered a way to use the picture of a person's iris to bypass iris-scanning security systems [4]. Such incidents raise new security challenges such as how to detect spoofing and to prevent reverse engineering.

Numerous techniques have been proposed to improve human identification and authorization methods. Some of these techniques investigated the emerging field of biometrics known as behaviometrics [5]. It has been hypothesized that individuals can be identified based on the characteristics of their behavioral traits, such as body posture [6], gestures, and keystrokes [7]. Biometric identification based on eye movements has emerged as a consequence of this assumption [8].

Current methods described in the literature for biometric identification using eye movements are typically limited by a low accuracy, thus preventing eye movements-based biometrics from becoming commercially viable. To address this limitation, research in eye movements investigated multimodal feature extraction methods to combine eye movements with static eye features such as iris matching [9] and distance between eyes [10].

Human eyes are very complex in their anatomical structure and constitute a rich source of information; therefore, more research is needed to take advantage of this complexity for biometrics. In the area of eye movement biometrics, it is still largely unknown which features are most useful for identifying users or which stimuli most influence the dynamic features of the eyes and their usability as a biometrical trait. For example, moving objects have been used mostly, whereas images and figures remain to be explored.

The present work investigates eye movements and iris features by testing several types of visual stimuli and comparing their viability for biometric identification in terms of identification accuracy. We also investigate the features of

the sphincter muscles in the iris that encircle and constrict the pupil, and the dilation muscles that expand the pupil, to suggest new dynamic features for biometric identification. This investigation correlates the described iris data with the stimulus used for exciting the iris. By proposing to combine the dynamic features of the eyes, which consist of the eye movements and the iris constriction and dilation behavior, we aim to improve the identification accuracy of state-of-the-art eye movement biometrics and to propose highly dynamic traits as an alternative to static biometrics traits**.** The work evaluates eye movements and iris features separately, and then performs feature fusion to evaluate their combined accuracy.

1.1 Biometric identification

Biometrics is a form of identification and access control that is based on characteristics and traits of individuals. Biometrics relies on identifying distinctive, measurable traits to label and describe individuals [11]. This method of access control emerged from traditional access control techniques that rely on using a personal token or memorizing a password. Biometrics is often categorized as *behavioral* and *physiological* [12], as elaborated hereafter.

Physiological biometrics is used for identifying individuals based on body traits. Normally, the body trait that is used as a biometric property includes the iris, face, fingerprints, and voice. Each physiological biometric method has its pros and cons thus, highly secure systems often use two or more traits. Fig. 1 illustrates the ranking of the most common biometrics [13]**.** According to the assessment criteria (i.e., intrusiveness, distinctiveness, accuracy, and cost) keystroke dynamics is the least costly biometric technique, while iris scanning is the most accurate and requires the least effort, and voice scanning is the least intrusive.

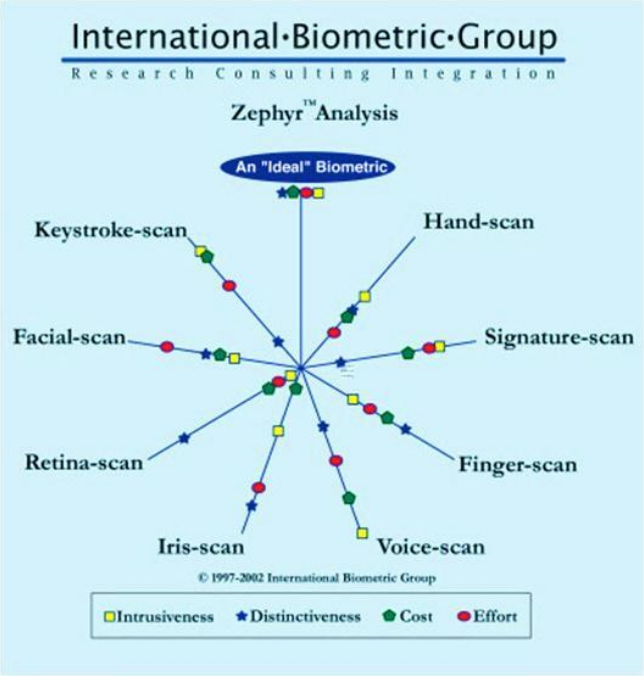

Figure 1. Static biometric ranking: The ideal biometrics will have the assessment factors as far from the center as possible [13].

Behavioral biometrics includes personal distinctive traits such as body movements (including eye movements) and actions (including typing patterns), all of which are associated with muscles. This category of biometrics is known to be very hard to use for fraudulent purposes [8]. Since this thesis investigates eye movements and other behavioral traits exhibited by the eyes, we examine the physiology of the components that form the eyes in the next sections.

1.2 Composition of the eye

1.2.1 Anatomy of the eye

Natural eye movement and pupil behavior occur when the eye adjusts the amount of light and its projection angle on the retina in order to be able to sense the visual information carried by the light**.** The light-sensitive area of the retina, known as the fovea, plays a vital role during this process because the light entering the eye must be projected on it. Naturally 50% of the vision happens at the foveal area, and when we move our eyes we essentially place the fovea region on the visual area that our brain needs to acquire [14]. Fig. 2 illustrates how the coming light from the image is projected on the fovea inside the eye globe.

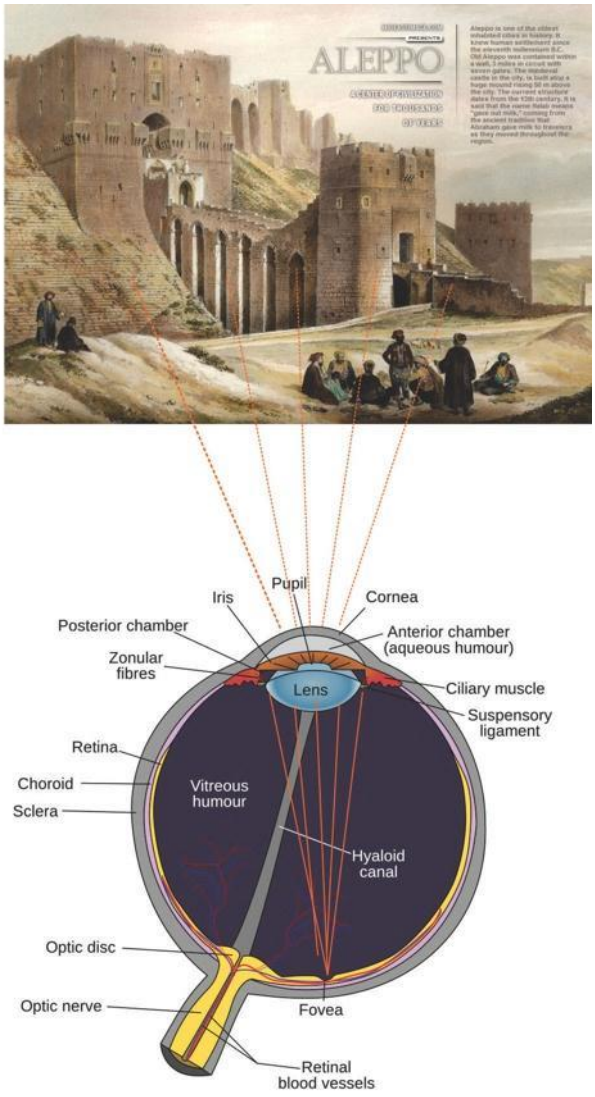

Figure 2. Projection of light coming to the eye is adjusted by the eye globe to be concentrated on the fovea [15].

Figure 3. F: foveal area (1-2°); PF: para-foveal area (2-5°); P: peripheral area (6-220°).

The human foveation process happens when the brain continuously sends nervous signals to the sensory-motor system to bring the image that we look at onto the fovea. For scene perception and processing of visual acuity, the retina is classified into three areas, namely the foveal area, parafoveal area, and peripheral area [16]. Fig. 3 illustrates how a human eye processes a scene. The foveal area (F) constitutes 1-2° degrees of the field of vision and forms the center of concentration in the eyes. The parafoveal area surrounds the foveal area and constitutes 2-5° degrees. The parafoveal area provides a distorted image to the brain that can also play a role in the vision process [17].

The eye globe is connected to a neural system that includes a complex set of nerves to move the eye and adjust its position to focus the light that is coming from the scene onto the retina [18], [19]. Fig. 4 shows the components of the muscular system that moves the globe. Those movements were found to be unique [9] because the neuronal signals and muscles are different in each person, which makes these components a potential biometric trait.

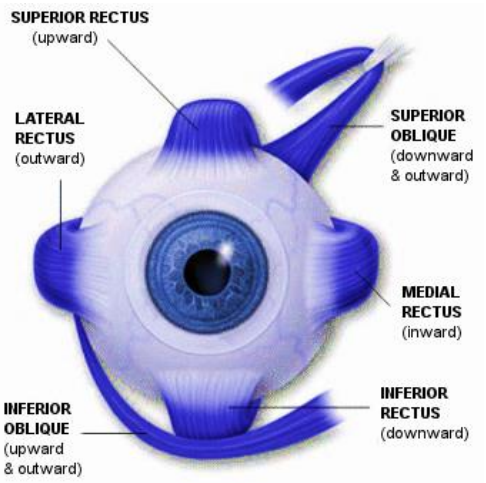

Figgure 4. The muscular system of the eye globe [20].

1.2.2 Anatomy of the iris

Pupil constriction and dilation occur when the iris adjusts the amount of light that should enter through the pupil to the retina [21]. The continuous tuning of pupil size is managed by a nervous system that regulates the tension and elasticity of the muscles that make up the iris. This process is highly linked with the stimulus that the

person looks at, and the activation of areas in the brain throughout the visual and cognitive tasks. The iris is made up of two types of muscles: sphincter muscles that encircle and constrict the pupil, and dilation muscles that expand the pupil [21]. The iris muscles are shown in Fig. 5.

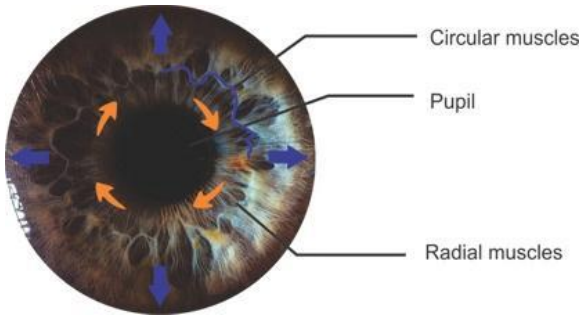

Figure 5. The circular and radial muscles of the eyes [21].

1.3 Eye movements and iris behavior

1.3.1 Eye movements

Natural eye movement is described by two types of motion: *fixations* and *saccades* [22]. A fixation is the sustaining of the eye focus on a single area [23]. A saccade is the rapid movement of the eye between any two given consecutive fixation points on the viewed scene. Saccades can be differentiated from fixations by determining whether the distance between consecutive fixations points is larger than a given threshold [24]. Figure 6 illustrates an example of two fixation points and a saccade between them.

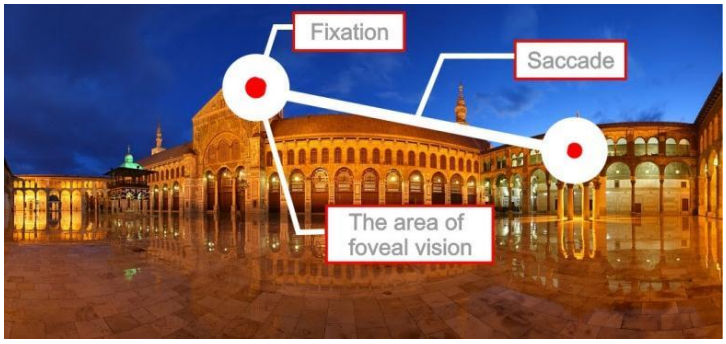

Figure 6. The eye behavior representation as fixations and saccades.

The circles in Fig. 6 characterize the fixation points on the shown image as an indicator of the visual attention, and the line between the circles represents the saccades between the fixation points**.**

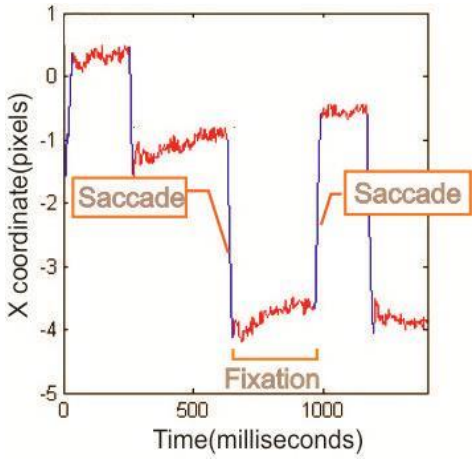

Figure 7. The measured eye movements, depicting saccades and fixations [24].

An illustration of the eye movement signal that shows the fixations and saccades is presented in Fig. 7. During fixations, the signal has a low frequency profile, and during saccades, the signal has a high frequency profile [24].

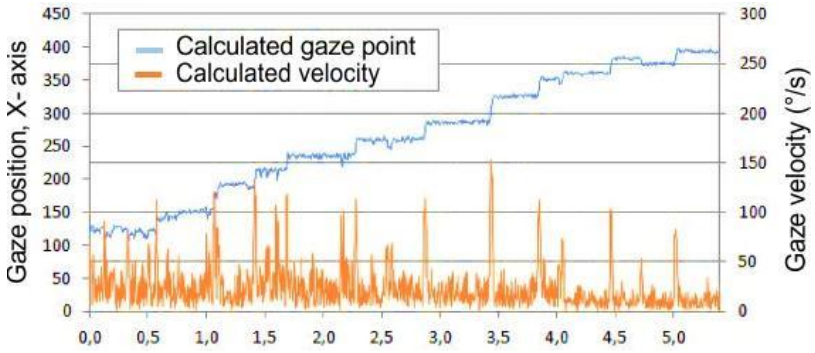

Figure 8. Variations in velocity between saccades and fixations [26].

The saccadic velocity, measured in visual degrees per seconds (°/s), is important for filtering and identifying saccades and fixations. Identifying eye movements is achieved by applying a *velocity threshold* between the eye's trajectories [25]. Fig. 8 illustrates the variation between eye movement saccades and fixations.

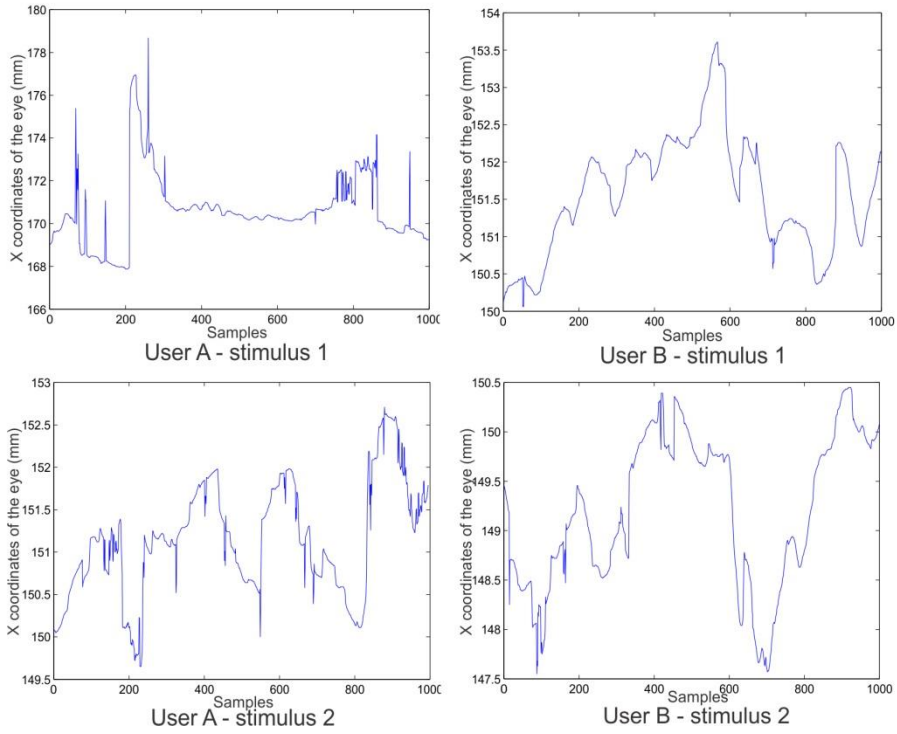

Figure 9. Eye movement behavior differences in two different users.

We conducted two preliminary experiments to investigate the behavior differences of the eye movements in two users A and B, where two different stimuli were presented, one in each experiment. A short-term window of the resulting signals is plotted in Fig. 9. We found that user A had an eye movement signal that was steep and had high frequencies; this behavior of the signal was caused by the saccades. In user B, the signal was smoother and had fewer fluctuations, as shown in the top two plots. When we repeated the experiment and introduced a new stimulus the same behavior in both signals occurred, as shown in the bottom plots. Such discrepancies can potentially yield unique eye movement features used to distinguish between individuals.

1.3.2 Iris dilation and constriction

The muscles in the iris control the size of the pupil by using sets of smooth muscles. These muscles continuously excite the pupil in response to the overall state of alertness or the mental workload required to perform a task, and in response to external factors [27], [28]. Pupillography has been employed in many perception experiments to monitor brain activities and the mental condition of the person, and

has been investigated by cognitive science researchers to determine the brain's cognition and processing level [29].

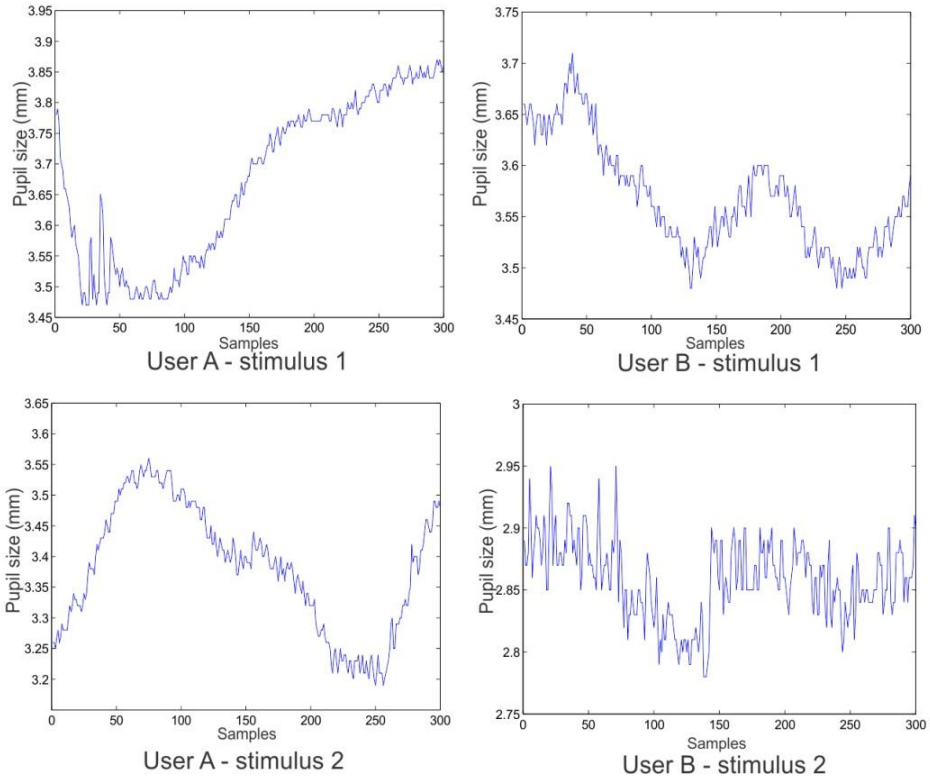

Figure 10. Pupil constriction and dilation behavior differences in two different users.

The muscles that make up the iris are unique to each person [30]; thus they might be responsible for unique contraction and expansion behavior. Moreover, there could be differences in the muscular properties of the iris in the left and the right eyes that can also make up a unique biometric trait [30]. In the preliminary experiments that we conducted earlier (described in the previous section), we measured the pupil dilation and constriction behavior by recording the size of the pupil during the experiments. Fig. 10 shows the plot of a short-term window of the pupil behavior in the same experiment. We can see in the plots that user A had a smooth signal but rapidly changed its frequency, which is an indicator that the pupil size changes are small, but the change occurs very rapidly. In the plot of user B, we can see that the signal is steep and has higher frequency. This is an indicator that the pupil size in the second user had a large range of size changes, unlike the first user. Such discrepancies are a potential biometric trait.

2 State of the art in eye movement biometrics

The natural behavior of the eyes has increasingly been gaining attention from the research community, in particular in relation to eye movements and pupil size. Eye movements can reveal information about the attentional and mental capacity of the person; therefore, eye movements were a subject of study in different fields of science, such as human computer interaction [31], cyber security [32], media research [33], and human identification [24]. Pupil constriction and dilation behavior has been a subject of study in brain cognition sciences. For example, it was found to be a good source of information to determine an individual's cognition and processing level [29]. In this work, eye movements as well as iris dilation and constriction responses are referred to as the dynamic feature of the eyes.

This thesis focuses on the development of a biometric system based on the dynamic features of the eyes. In this section we provide a review of the related work in human identification using the dynamic features of the eyes. The development of eye movement biometrics comprises four fundamental areas of research, namely: identifying the stimulus that must be used to excite the eye movements; extracting the eye movement features that can make up a biometric trait; selecting the techniques used to adequately process the features; and choosing the best machine learning approach for classifying users based on the resulting features. The following sections present existing work in the literature of eye movement biometrics organized according to these four fundamental areas.

2.1 Visual stimuli methodology

Human eyes exhibit different movements that indicate the attentional and mental capacity of the person in relation to the visual stimuli. Those movements are not random and are influenced by certain factors including cognitive aspects such as attention and memory [34]. During some cognitive processes such as attention to the visual scene**,** the brain guides the eyes to acquire informative visual components [35]. The past work in the literature has deployed eye movements in biometrics primarily focused on two types of visual stimuli: static and dynamic stimuli. A static stimulus is a visual scene that does not change in time (e.g., images and texts). A dynamic stimulus is a visual scene that changes in time (e.g., movies and animated pictures).

2.1.1 Static stimuli

Text-based stimuli

Reading activates a series of eye movements known as the scan path, which is the sequence of eye fixations and saccades made when someone looks at a visual scene or reads a text [36]. Holland et al. [37] have proposed a method for human identification based on the scan path using a text as a stimulus. The authors have reported the eye's trajectories of the participants during a short reading task and analyzed quantitative properties of the scan path such as the number of fixations and the average duration of each fixation. Fig. 11 illustrates an example of the scan path that the authors reported from a participant in their study.

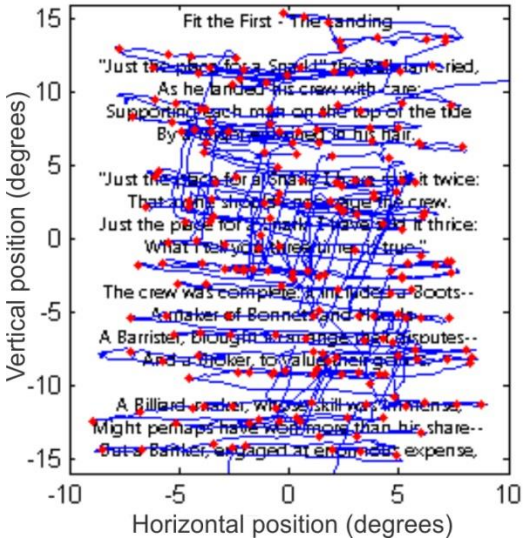

Figure 11. An example of a text-based stimulus and the scan path followed by the eyes when reading [37].

The authors concluded that individuals tend to repeat certain scan paths during repeated viewings of the same text-based stimulus. The variations in the scan path between individuals and the path's similarity in the same person might make the text-based stimulus a promising candidate to excite the behavior of the eyes for eye movement biometrics.

The findings of Noton and Stark [36] were supported by Holland et al. [37], where the authors found that the scan path made by the eye movements of a subject during reading was repeated in 65% of subsequent text readings. These findings suggest that the text-based stimulus can be a good method to investigate for eye

movement biometrics. Moreover, a text-based stimulus is highly usable since reading is a very common activity.

However, the authors did not discuss whether the language of the text and the reading skills of the individuals had any influence on the findings. For example, individuals might have a different scan path when the text is familiar and easy to read. Also, previous studies did not report whether the learning factor, which means to become familiar with the task**,** had any effect on the scan path. These disadvantages make the text-based stimulus a priori a less efficient method to implement for a commercial eye movement biometrics application. Therefore, we did not investigate text as a stimulus in the experiments that we conducted. Instead, a task-independent approach is investigated in this work, which will solve the problem of the learning effect.

Image-based stimuli

Bednarik et al. [38] have investigated the images for exciting the eye movements of individuals for biometric identification. The authors have also studied other stimuli such as a text and a moving object. The study did not report whether images alone could be a good method for eye movement biometrics since all stimuli were studied together without being compared for their effect.

Komogortsev et al. [9] investigated the use of static images as a stimulus for eye movements; They used a complex pattern image known as Rorschach inkblots [39] as illustrated in Fig. 12.

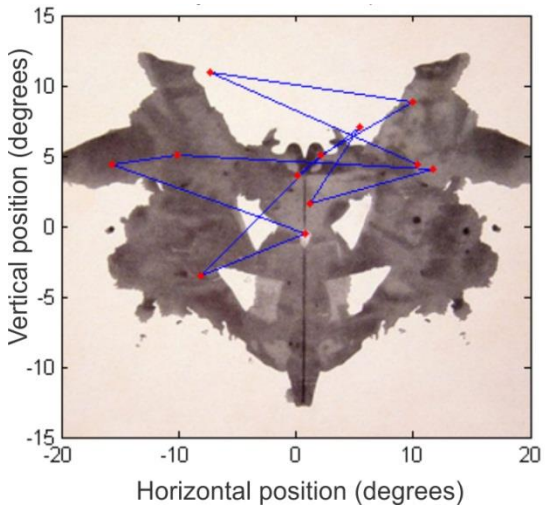

Figure 12. An example of an image-based stimulus [9].

Although the authors concluded that the inkblots could be used for eye movement biometrics, they did not investigate other types of images and especially more common ones. Moreover, the inkblots are used in psychological tests in which the subjects' acuity of the inkblots is recorded and analyzed, and might therefore be a less reliable stimulus for most common individuals [39]. While the effect of text stimuli and the characteristics of the scanpath are well-known, the influence of different types of image stimuli remains largely unexplored and requires further investigation. The work presented in this thesis proposes the use of general-purpose images for exciting the eye movements and compares the images to other stimuli to validate images viability for biometric identification.

2.1.2 Dynamic stimuli

Jumping point stimuli

The work of Kasprowski and Ober [24] was the first attempt to study eye movements as a personal trait for biometric identification. The authors designed a 3x3 matrix of yellow dots as shown in Fig. 13 and used this stimulus to excite the movements of the eyes for biometric identification.

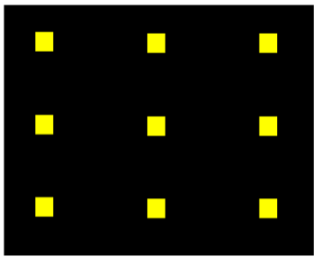

Figure 13. An example of jumping dot stimulus [24].

Each dot in the matrix flashed one after the other for 550 ms to create an animation of a jumping point, as illustrated in Fig. 14.

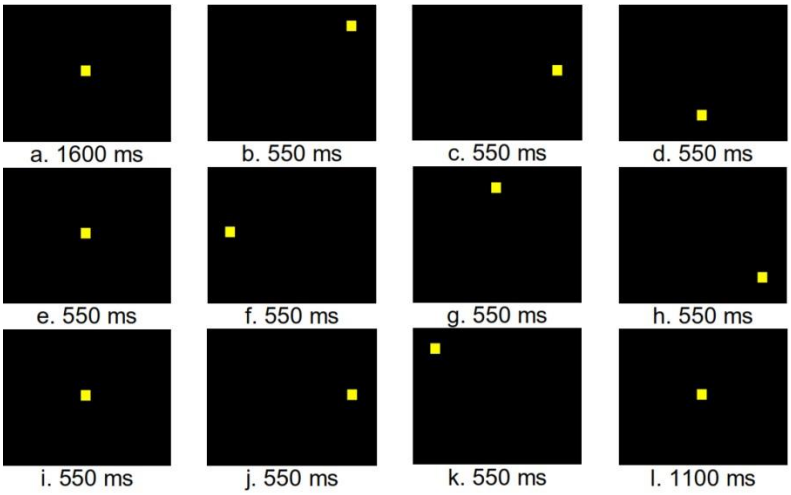

Figure 14. The sequence of dot matrices creating a jumping point animation [24].

The jumping point stimulus has been widely adopted by the researchers for eye movement biometrics. Komogortsev et al. [40] investigated a similar approach when they conducted a study to evaluate the feasibility of using eye movements for biometric identification. The authors presented a jumping point stimulus for exciting the movements of the eyes. The purpose of the experiment was to find the movements that could be used for biometric identification by using a simple dynamic stimulus such as a jumping point.

Although the authors proposed a jumping point as a stimulus to find a simple way to excite eye movements, this stimulus required full attention from the individuals in order to follow the dot, and limited the individual's freedom in natural viewing. Furthermore, the jumping dot stimulus is hard to deploy as a general-purpose stimulus in commercial applications, especially those that require an ongoing validation of the user identity. In the experiments that we conducted, we tried to find more robust stimuli than the jumping point, for example, stimuli that require less attention from the user.

Movie stimuli

Kinnunen et al. [41] proposed using a movie as a stimulus for exciting the eye movements for biometric identification. The authors proposed this dynamic stimulus to excite the movements of the eyes because watching a movie is not correlated with a specific task or instructions, and movies as a stimulus method can be used for stealth identification. In their study, the participants were required to watch a 25-minute

movie that was presented on an eye tracker screen. Then, the eye movement signal was segmented into short-term signals to determine how much time was sufficient for collecting usable eye movement data for biometric identification. Fig. 15 shows an example of the overall eye movement scan path on the movie (right) and a short-term sample of the scan path (left).

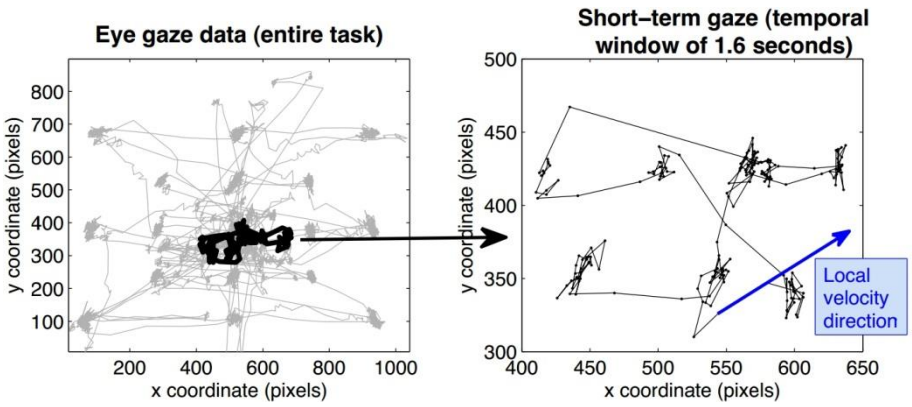

Figure 15. Representation of eye movement when watching a movie stimulus [41].

The authors found that at least 5 minutes of movie watching was sufficient to collect usable eye movement data for biometric identification.

Although the authors' attempt to use a movie as a stimulus was found feasible for eye movement biometrics, it is impractical and requires users to watch the stimulus for a long duration. Therefore, the use of movies as a stimulus was not investigated in this thesis and instead we looked for more practical stimuli as elaborated in the next sections.

2.2 Eye-movement features

The movements of the eyes are generated by complex anatomical components, which include six extraocular muscles (EOMs) that move the eye globe. These movements are subject to the force-velocity relationship of the muscles, and the resistive factors found in tissues surrounding the eye globe [42]. The eye movement is described by two types of behavior: fixations and saccades as described in Section 1.2.1.

This section presents past research in eye movement biometrics that is related to the anatomical properties of the eye movements such as the oculomotor system,

and the behavioral properties that are generated by other complex factors such as the neuronal control and the brain.

2.2.1 Anatomical characteristics

A few studies have investigated the complex anatomical structure of the oculomotor plant (OP) for biometrics. OP is responsible for generating eye movements that are unique in individuals and can be used as biometric features [40] [42]. OP components include the eye globe and its surrounding tissues, EOMs, and other tissues [21].

OP characteristics were proposed as a method for biometric identification by Bednarik [38], including: length tension, series elasticity, passive velocity, and relationships of force-velocity.

Komogortsev et al. proposed a mathematical model to estimate eyes' OP values by finding the differences in the eyes' positional signal, and by comparing these values against the generated saccades to produce optimized OP values [42]. The authors concluded that the biometric identification based on the OP characteristics of the eyes is a promising method for biometric identification.

The proposed anatomical characteristics in the previous work require advanced eye tracking technology with a high sampling rate, which can only be found in advanced research laboratories. The sampling rate of the eye tracker represents the number of captured eye movement samples per minute. Thus, the higher the sampling rates the better the accuracy of the captured eye movements. The eye tracker that was used in this thesis to report the movements of the eyes is a commercial product with a lower sampling rate, which makes investigating the OP characteristics hard. Therefore, we investigated the behavioral characteristics, as described in the next section, since the OP influences the behavioral characteristics in terms of the velocity and acceleration of the eye movements.

2.2.2 Behavioral characteristics

The behavioral characteristics of eye movements can be unique and individualized [38], [41], [43]. They are mainly brain-guided movements during the visual activities and perceptual process of acquiring the visual scene. These characteristics are a very rich source of information and they can produce a rather large number of features [43] such as the scan path and subsets of behavioral features

which include horizontal amplitude of saccades, vertical amplitude of saccades, saccades velocity, fixation count, fixation duration, and scan path length [9].

Kasprowski et al. [24], [44] investigated the behavioral characteristics of the eyes during the visual activities and constructed three feature sets for biometric identification. The features included eyes' average velocity, direction and distance to the stimulus, and distance between eyes [38].

The behavioral eye movements that were investigated in the literature were the first order derivative of eye movements as will be explained in Section 3.4. In this thesis, we will investigate the behavioral features that were investigated in the literature as well as the second-order derivative of the behavioral features such as the acceleration and peak acceleration of eye movements.

2.3 Pupil constriction and dilation as a biometric trait

Pupil constriction and dilation behavior, which refers to the size variations of the pupil, has been a subject of study in brain cognition sciences. Recently, some work was done to investigate the feasibility of using the size of the pupil for biometrics [38].

Bendarik et al. [38] were the first to investigate pupil size as a biometric trait by combining it with the velocity of eye movements to increase the identification accuracy of the eye movement biometrics system. The authors found that combining the pupil size with the eye movements increased the overall accuracy of the system.

Bednarik et al.'s work was the only attempt to investigate the pupil as a biometric trait, to the best of our knowledge. However, the extracted features were the size of the pupil, which might not serve as a biometric trait when a large group of users are investigated for their pupil size. That is because the size of the human pupil is limited to a small range of millimeters [45].

In this thesis, we will investigate the pupil constriction and dilation behavior for biometric identification by proposing to use features such as the acceleration and velocity of the pupil size changes, as elaborated in Section 3.4.

2.4 Extracting eye movement features

The characteristics of the eye movements that were investigated in the literature, as explained in the previous section, required a feature extraction process

where usable traits from eye movement characteristics could be extracted to be used in biometrics. This section focuses on the feature extraction techniques that were proposed in the literature.

The past work in eye movement biometrics has used feature extraction techniques similar to those employed in fingerprint and hand geometry biometrics. Those techniques included Principal Component Analysis (PCA), Linear Discriminate Analysis (LDA), and transform methods such as the Discrete Fourier Transform (DFT) and Continuous Wavelet Transform (CWT).

PCA has been investigated by Bednarik et al. [38] and Kasprowski et al. [46] for feature extraction in eye movement biometrics. PCA has the main advantage of being easy to use [47]. In this thesis, we also investigate PCA as feature extraction technique because of the many advantages that it offers. For instance, it allows our multivariate features to be represented by a smaller number of variables [24].

Linear discriminate analysis (LDA) has been investigated by Klami et al. [48] and Holland et al. [37] for eye movement feature extraction. LDA requires many more calculations than PCA and since in our work we investigated many eye movement and iris characteristics, feature extraction time was important. Therefore, the LDA technique was not investigated.

DFT has been investigated in the literature for analyzing the frequency patterns of eye movements and extracting the hidden features in the original eye movements such as the micro-movements [38], [46]. The micro-movements of the eyes are a behavioral trait that is caused by the osculation of the eyes during fixations. Individuals' eyes might have different micro-movement behavior that can be considered a biometric feature [46]. The main disadvantage of deploying DFT for extracting the features that are hidden in the eye movement characteristics is that it requires good quality of signal, which is extracted from a high-grade eye tracker. That is because eye trackers with low sampling frequencies, such as the one used in our study, have residual noise that cannot be filtered, making noise appear similar to the micro-movement feature.

The Continuous Wavelet Transform (CWT) has been investigated by Bulling et al. [43] for extracting eye movement features such as fixations and blinks. CWT has an advantage over DFT due to its ability to perform more feature extraction from the eye movements that are collected from eye trackers with a lower frequency [43],

[46]. In this work, we used a much simpler and faster technique to extract eye movement features as elaborated in Section 3.4.

Other feature extraction techniques such as the Minimum Spanning Tree (MST) have been used to extract eye movement features for biometrics. MST has the advantage of transforming the raw data of eye movements into smaller regions that can be computed using statistical test methods to extract the features [49]. For example, Rigas et al. [50] applied MST to the raw eye movement characteristics to create small templates of eye movement fixations and saccades. The templates' mean and covariance were computed and compared for finding eye movement features for biometrics. Holland and Komogortsev [37] also investigated MST for extracting eye movement features; however, the authors used a different statistical method known as "weighted mean fusion" to produce new eye movement features for biometrics. Using MST with statistical techniques to extract eye movement features was very useful for extracting features for biometric identification and yielded low error rates, as will be discussed in the next section. In this thesis, we investigated a similar technique to MST, yet simpler. Our technique was based on segmenting the saccades and fixations and applying statistical techniques to the segments such as mean and variance, as elaborated in Section 3.4.

Feature extraction techniques that are commonly used in voice recognition biometrics such as the Gaussian Mixture Model (GMM) and Universal Background Model (UBM) were investigated by Kinnunen et al. [41]. GMM and UBM were used by the authors to extract eye movement features for task-independent biometric identification. GMM and UBM require long computation times as well as a large number of raw eye movement samples, which makes them hard to implement for general-purpose eye movement biometrics.

2.5 Classification and evaluation of eye movement features

In the previous work in eye movement biometrics, many classification techniques were used to classify features of eye movements and build a machine learning model. However, four classification techniques were the most commonly investigated, namely: Support Vector Machine (SVM) [50], K-Nearest Neighbor (KNN) [38], Hotteling's/T-square test [24], [51], and the C45 decision tree [24], [44].

Five factors were used to estimate the performance of human identification via eye movements: 1) False Acceptance Rate (FAR); 2) False Rejection Rate (FRR);

3) Half Total Error Rate (HTER), which is the average of both FAR and FRR; 4) Equal Error Rate (EER), the point where FRR equals FAR; 5) recognition accuracy, which is the ratio of the number of records classified correctly to the total number of records (also equal to 1 – FAR – FRR). Table 1 shows a summary of the techniques used to evaluate biometric identification using eye movements.

Table 1. The error rates of biometric classification tests in the literature. An '_' means that the results were not provided by the authors.

	Classification technique	*FAR*	*FRR*	*HTER*	*EER*	*Recognition accuracy*
Kasprowski [46]	NB C45 C45.1 SVM	40.88% 12.43% 10.37% 10.80%	21.27% 45.79% 48.36% 43.60%	31.08% 29.11% 29.36% 27.20%	_	_
Komogortsev et al. [9]	Hotteling's Pairwise Distance Comparison (PDC), Gaussian Cumulative Distribution (GCD)	_	_	37% 36.3% 33.6%	_	_
Komogortsev et al. [42]	Hotteling's/T-square test	_	_	15%	_	_
Holland [37]	Similarity scores	_	_	_	30%	_
Rigas [50]	KNN (K= 1and 3)	_	_	_	30%	_
Bednarik [38]	KNN, Leave-one-out cross validation, Fusion weight	_	_	_	_	40-90%
Kasprowski et al.[44]	2D histogram speed and direction, SVM	_	_	_	_	97.55%

The lowest error rate in eye movement biometrics was the Half Total Error Rate (HTER) of 15% in the work of Komogortsev et al. [42], while the highest recognition accuracy (97.5%) was found in the work of Kasprowski et al. [44]. However, recognition accuracy is not a comparable metric that can be used to determine the accuracy of the biometric system. Thus, metrics such as HTER and EER must be provided to enable us to evaluate the obtained results.

The error rate achieved in the investigated work clearly reflects the challenges yet to be addressed prior to the adoption of a standalone system that would rely solely on eye movements for human identification and authentication. Improvements are necessary in several areas, including: extracting features that are more purposeful for human identification (as those features investigated so far have yielded relatively low

identification accuracy), creating general-purpose methods for everyday identification activities, and conducting experiments with a large number of users (although this is obviously difficult due to the resource required). Our work aims at addressing these issues and expanding current research in eye movement-based biometrics by investigating a wide range of eye movement features, and incorporating other dynamic features found in the eyes. We also propose to investigate various stimuli and study their effect on the dynamic features of the eyes for classification purposes in order to identify stimuli that can be used in common identification activities.

2.6 Eye tracking technology

Eye tracking is the procedure of monitoring and reporting the natural behavior of the eyes. Eye tracking technology is increasingly applied to research in several areas, such as human computer interaction [52], [53], cognitive sciences that study the influence of the stimulus on the human brain [54], and in studying the eye area of interest during phishing attacks [55]. Various eye tracking technologies have been developed for tracking the movements of the eyes. These technologies include Infra-red Corneal Reflection Oculography (IROG), Electro-Oculography (EOG), and Video-Oculography (VOG), explained hereafter.

2.6.1 Electro-oculography

The eye globe is a dipole with a positive pole at the cornea and a negative pole at the retina. The potential difference generates a steady electric potential field that can be measured to determine the movement of the eye globe. In order to measure the electric field, two pairs of electrodes must be placed on the skin surrounding the ocularcavity area in the opposite directions of the eye. This technique is known as the Electro-Oculogram (EOG). The EOG reports the horizontal and vertical movement components of the eyes, allowing them to be measured as signals that range between 5 μv/° to 20 μv/° [51].

The main disadvantage of EOG is that the electrodes are required to maintain direct contact with the skin surrounding the eye, which makes this technique very intrusive. Moreover, dry skin or poor electrode placement can undermine the readings. EOG, however, remains the lowest cost eye-tracking method, making it highly affordable for eye tracking research.

2.6.2 Video-Oculography

Video-Oculography (VOG) eye tracking technology uses the rotation and translation of the corneal reflection of the light to estimate the position of the eyes. Infra-red can be used as a source of light and its reflection from the eyes can be captured with a regular CCD camera that is mounted on the head like a helmet.

The main disadvantage of VOG is the installation process that requires a person to wear the helmet and adjust the position of the camera to capture accurate readings of eye movements [56]. VOG does not require direct contact with the skin surrounding the eyes, which makes it a less intrusive eye-tracking method than EOG.

2.6.3 Infra-red Corneal Reflection Oculography

Infra-red Corneal Reflection Oculography (IROG) is a widely available commercial eye tracking technology. It takes advantage of a technique using the corneal-reflection and pupil-center to estimate the position of the eyes. This technique is quite simple and can be constructed by using a camera and an IR light source. The IR light generates bright pupil and dark pupil images that are sensed by a camera or sensor [57]. When the light enters the retina, it is reflected back and appears to the camera as a bright spot that can be tracked and identified by image processing methods [52].

3 Methodology in investigating the eyes' dynamic features

This chapter presents the methodology that was employed to investigate the human identification problem using the dynamic features of the eyes. The following section presents a brief overview of the approach used to build the biometric identification system. Later sections describe the participants and the experimental procedure, the investigated stimuli for exciting the dynamic behavior of the eyes, the methodology used for processing the recorded data by the eye tracker, and the approach of extracting the dynamic features of the eyes from the processed signal.

3.1 System overview

The approach adopted in this work considers the behavior of the human eyes as an input comprising user-specific features. By using a visual scene as a stimulus to excite the eye movements, non-intrusive eye tracking technology can record the behavior of the eyes as sequences of pixel coordinates and present them as a time signal. The proposed system takes this signal as an input and extracts features such as acceleration and velocity. A classifier is trained using the created features and a machine learning model is built. An individual can be identified based on the eye movements for various security applications. The overall goal of the biometric system that was built in this work is to recognize individuals and validate their identity based on their eyes' behavior. This identification is achieved non-intrusively and without using a specific task or stimulus. To validate the system, the error rate was computed and compared with the similar values from published studies in eye movement biometrics. The steps followed to create our system are illustrated in Fig.16.

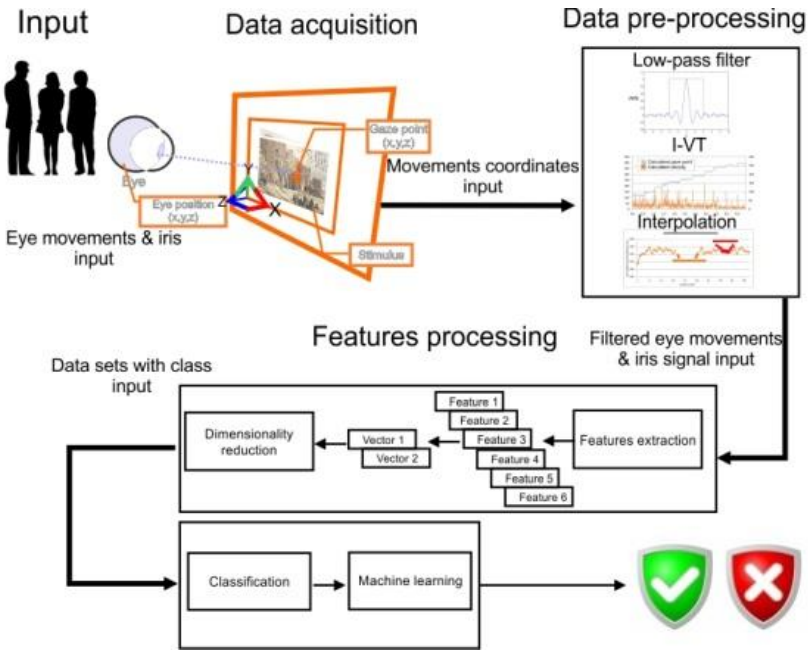

Figure 16. An overview of the system architecture.

3.2 Eye tracking apparatus

The research presented in this thesis employed IROG eye tracking technology by using a Tobii T120 [26] eye tracker with a sampling rate of 120 Hz for simultaneously recording the movements of the eyes and the pupil size. The tracker recorded eye movements in pixels on a 2D plane as coordinates on the tracker's display screen, where the origin point of the recorded eye positions was located at the top left corner of the display (as shown in Fig. 17), and records the pupil size in millimeters.

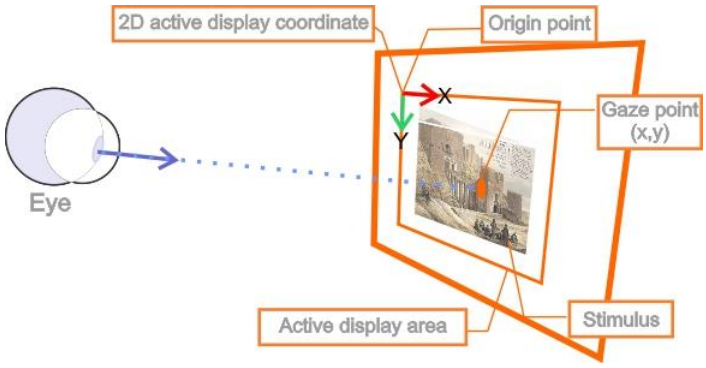

Figure 17. 2D (X and Y) plane of eye gaze points on the image stimulus.

The main advantage of using the IROG technology in this work is its non-intrusiveness and ability to provide high precession eye movements and pupil size readings. However, IROG technology is expensive, especially versions with higher sampling rates.

The Tobii eye tracker estimates the position of the eye gaze by sending a beam of infra-red light in the opposite direction of the eye tracker screen. A small but sufficient amount of infra-red light is reflected on the user's cornea and received by the built-in sensors of the eye tracker, which estimates the position of the eyes based on the reflection angle. Fig. 18 illustrates this process, while Table 2 provides the technical specifications of the eye tracker.

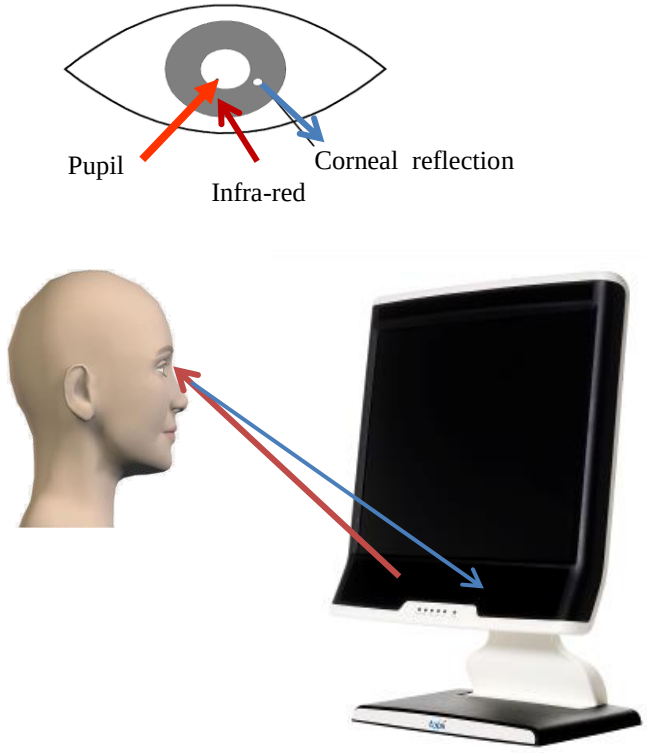

Figure 18. An overview of the system architecture.

Table 2. Technical specifications of the eye tracking apparatus used in the study [60].

Data rate	120Hz
Accuracy	0.5 degrees
Drift	0.1 degrees
Spatial resolution	0.3 degrees
Head movement error	0.2 degrees
Head movement box (width x hight)	30 x 22 cm at 70 cm
Tracking distance	50-80 cm
Max gaze angles	35 degrees
Latency	maximum 33 ms
Time to tracking recovery	typical 300 ms

The reported pupil size and the X and Y positions of the left and right eyes, were extracted using the Tobii Software Development Kit (SDK) [61] and exported to Matlab. Fig. 19 shows part of the raw data recorded by the eye tracker.

GazePointIndex	GazePointLeftX	GazePointLeftY	GazePointRightX	GazePointRightY	Pupil size Left	Pupil size Right	ValidityLeft	ValidityRight
1	348	984	363	978	3.35	3.25	0	0
2	326	992	343	993	3.34	3.24	0	0
3	328	998	334	995	3.33	3.22	0	0
4	326	999	335	997	3.33	3.23	0	0
5	323	997	335	994	3.32	3.22	0	0
6	323	996	328	995	3.31	3.22	0	0
7	321	1000	329	992	3.31	3.22	0	0
8	321	1006	328	990	3.29	3.19	0	0
9	325	1007	332	996	3.29	3.18	0	0
10	328	1002	339	993	3.3	3.18	0	0
11	325	1008	333	995	3.3	3.2	0	0
12	324	1014	331	993	3.29	3.21	0	0
13	321	1011	333	999	3.3	3.2	0	0
14	322	1005	330	1000	3.29	3.18	0	0
15	331	1005	328	995	3.29	3.17	0	0
16	329	1015	334	994	3.28	3.17	0	0
17	321	1011	335	992	3.26	3.18	0	0

Figure 19. A sample of the data recorded by the eye tracker.

3.3 Participants and procedure

The study was approved by the Institutional Review Board (IRB) of the American University of Sharjah, and by Zayed University where the experiments were conducted, and received ethical clearance. Informed consent was obtained from participants, who had the right to stop and leave the experiment at any time.

A total of 22 subjects volunteered to participate in the experiments (15 females, 7 males). Their ages ranged between 17 and 52, with a mean of 20.4 and standard deviation of 5.2. The eye movements and pupillary behavior data was

collected from the participants using one eye tracking device that was adjusted for each participant to maintain a distance between the subject and the screen within 55 mm and 62 mm, and with a maximum of 2° degrees of error in the visual angle as recommended by Komogortsev et al. [40]. Fig. 20 shows the setup of the eye tracker while a participant was conducting the experiment.

Figure 20. The setup of the eye tracker apparatus in the laboratory.

The eye tracker recorded the eye movements and the pupil size with a 100% accuracy indicating that all samples (eye recordings) were acquired. A lower accuracy indicated that the eye tracker did not detect the presence of the participant's eyes for a period of time due to blinks, head movement, or other temporal obstacles. For example, when the participant blinked or looked outside the screen that was presenting the stimulus, the eye tracker did not report any eye movements. During the experiment, poor eye tracking performance was also found in one participant that had long eyelashes, which distorted the infrared beams that were used by the eye tracker to determine the pupil position. Poor recording accuracy was also found in four

participants who used eye glasses infra-red reflection. We excluded recordings that had accuracy rates below 80% to maintain reliable eye-tracking data. After exclusion, data recording from 17 participants remained, 11 females and 6 males, with ages ranging between 17 and 50, with a mean of 21.1 and standard deviation of 4.9. Each participant undertook four experiments as described in the next section.

3.4 Performance metrics

The performance of the proposed biometric system is measured through a number of parameters and summarized by a single variable which is the Half Total Error Rate (HTER) [57]. The HTER refers to the midpoint of errors between the False Acceptance Rate (FAR) and the False Rejection Rate (FRR) [57]. In statistics, FAR and FRR are referred to as the Type I and Type II errors, respectively [58]. We also provide the percentage of correctly classified instances to give insight into what fraction of the provided data was correctly classified.

3.5 Methodology for designing and using the visual stimuli

The stimuli in our experiments were designed to test the feasibility of eye movement biometrics for general-purpose identification and authorization. We took two parallel pathways in developing the visual stimuli to determine the best stimulus for exciting the dynamic features of the eyes for building a biometric system. We called the first pathway the *task-driven stimulus,* and the other pathway the *task-independent stimulus.* Both pathways are explained in detail in the next section.

The study scenarios involved four stimuli that were chosen to represent a much broader set of stimuli that could be used for general-purpose eye movement biometrics. The experiments that are elaborated in the next sections are as follows. The first experiment examined a task-driven stimulus that required the participants to replicate a task, for instance drawing a given shape. The second experiment examined a task-driven stimulus that consisted of replication and redrawing of memorized shapes such as a password pattern. The third experiment examined a graph-based stimulus that was also task-driven and required participants to trace the plots of the graph with their eyes. The fourth experiment examined task-independent stimulus that consisted of images such as a natural scene.

3.5.1 Task-driven stimuli

We call a stimulus "task-driven" when it is related to a task that is required to be accomplished, for instance drawing a pattern or replicating a shape by moving the eyes. Task-driven stimuli have no time limit; thus the participants decide when the task is finished. The following section describes the stimuli and the task used in each experiment.

Experiment 1. Short term cognition

Short-term cognition is a field of study in cognitive science [62], [63]. Visual short-term cognition is defined as the ability to briefly retain a small amount of visual information such a shapes and colors, and make the retained visual information active and available for a short period of time [62].

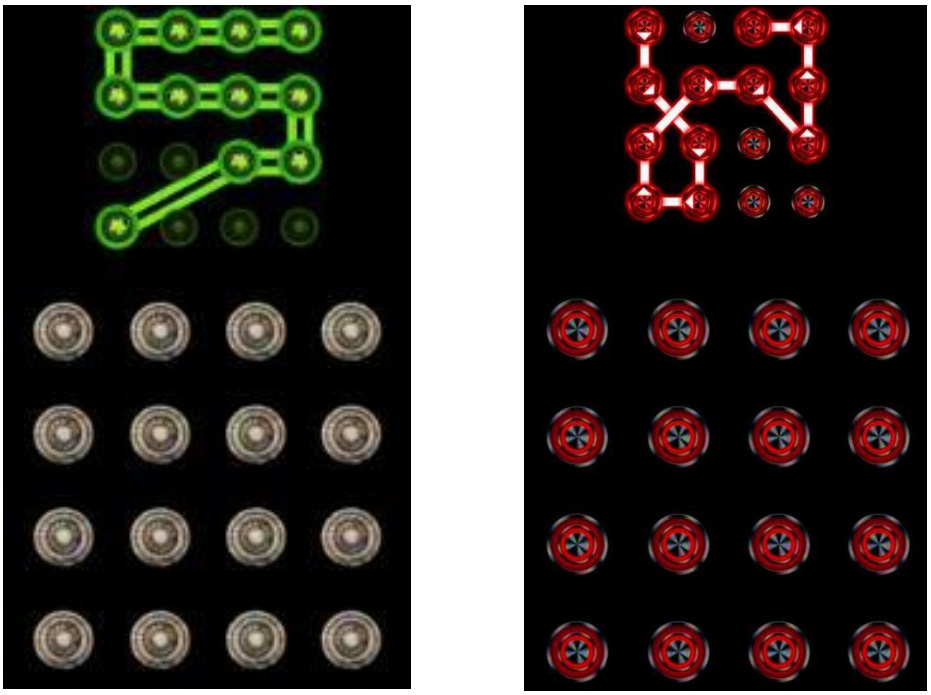

(a) (b)

Figure 21. The short term cognition stimuli used in Experiment 1. Users were required to replicate the shape (top), on the pad (bottom).

In the first experiment, the stimuli consisted of two high-resolution shapes and a 4x4 dot-pad that had a full screen size (1280 x 1024) as shown in Fig. 21. These types of stimuli were chosen for two reasons: to hypothesize whether it is possible to extract usable dynamic features from the participants' eyes for biometric

identification using short and simple tasks, and to study the response of the eyes to stimuli and activities that require short term cognition. We proposed to present two stimuli in order to increase the number of acquired samples and extract an adequate amount of dynamic eye movement data that could be used for biometric identification.

The 22 participants were advised to look at the screen and follow the experiment instructions. The first task required them to look at the shape shown in Fig. 21 (top) and to replicate it on the pad that is shown in the bottom. Participants were asked to complete their tasks in one trial and press the space key on the keyboard after completing the experiment.

Experiment 2. Long-term cognition

Long-term cognition is another well-established subject of study in cognitive and neural sciences [64]. Visual long-term cognition is the process of retaining visual information such as shapes and colors and making it available for a long period of time. Such activities are commonly practiced by people on a daily basis.

Visual stimuli were 4 x 4 dots with consistent low luminance and a black background. Two images were presented with a 1280 x 1024 resolution, as shown in Fig. 22. This stimulus was chosen for two reasons: a pattern lock screen is a password interface element used by various operating systems in smart touch phones, and it allows studying the response of the eyes to activities that require long term cognition.

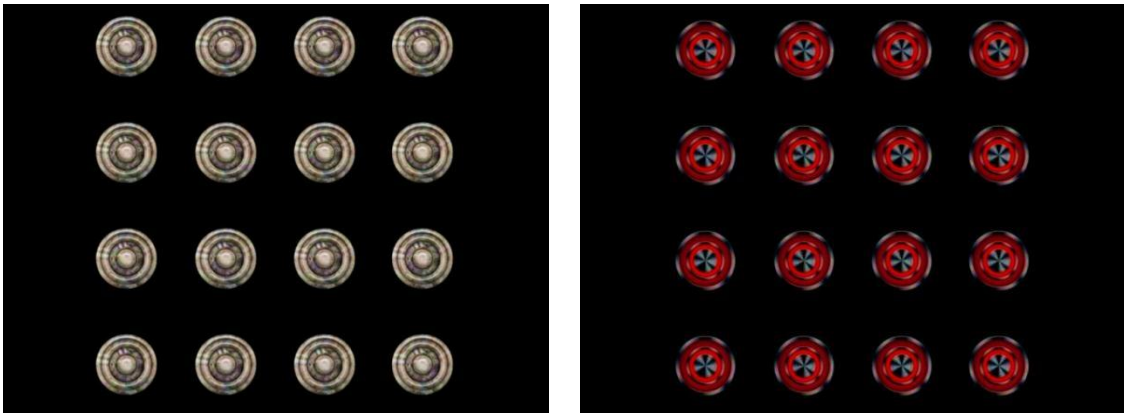

(a) (b)

Figure 22. The long-term cognitive stimulus that was used in Experiment 2.

Participants were asked to choose a shape that could connect at least 7 dots in the dot pad shown in Fig. 22. Each participant had to memorize and practice two different shapes before undertaking the experiment. The stimulus shown in Fig. 22 was presented to all participants on two consecutive slides; a and b, respectively. Each viewed stimulus continued as long as the viewer did not press the space bar, which is an indication that the task was completed.

Experiment 3. Simple activity

The stimulus that was presented in the third experiment was designed to study the eye movements during simple tasks**.** The stimulus consisted of three plots in one figure, as shown in Fig. 23, to provide more time to collect an adequate amount of eye movement data from the participants.

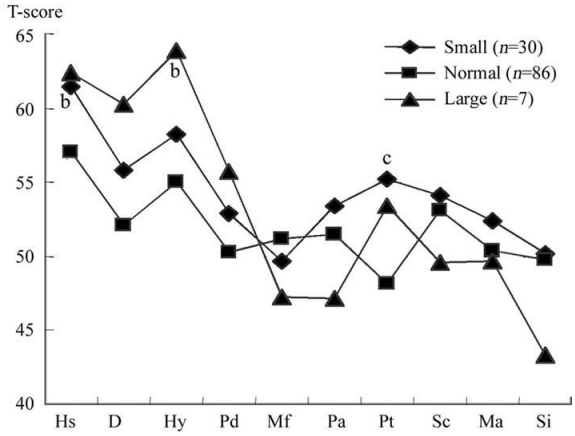

Figure 23. The stimulus that was presented in Experiment 3.

The plot stimulus has the advantage of being easy to generate by the device that will authenticate users based on their eye movement biometrics. Moreover, this type of stimulus is common and users might find it easy to simulate.

Participants were asked to trace with their eyes each of the three plots during the experiment, and to press the space bar after they traced the plots.

3.5.2 Task-independent stimuli

The task-driven stimuli presented in the previous section assumed that the same or similar tasks appear in training and testing of eye movements for user identification. This approach has the advantage of identifying the user with a

relatively low margin of error as elaborated in Section 4. However, when eye movement biometrics is deployed in scenarios that require repeated authentication such as security, the user is forced to perform tasks that become learned. The learning effect in eye movement biometrics has not yet been studied, to the best of our knowledge; however, it has been found that the learning effect has a negative impact on the classification accuracy in other types of behavioral biometrics such as keystrokes [65], [66]. The task-independent stimulus can solve this issue by presenting to the users stimuli that require neither prior knowledge nor a specific activity to be performed. For example, images are considered task-independent stimuli because the users can freely watch them without having to follow any instructions. However, if the user is instructed to look at or search for particular areas in the image, the image is considered a task-driven stimulus. One of the advantages of using this type of stimulus is that they are common and can be used for many applications such as stealth identification.

Experiment 4. Task-independent

The stimuli in Experiment 4 were two high-resolution images that were presented in a full screen size. The image-based stimuli were chosen as stimuli for determining images' usefulness for extracting eye movements and pupillary response features for biometric identification. Participants were asked to look at the images that were displayed but without advising any specific task. The image-based stimuli are shown in Fig. 24.

(a) (b)

Figure 24. The task-independent stimulus that was presented in Experiment 4.

Participants were instructed to look at the displayed image, but no particular guidance was given**.** Each image was presented for 20 seconds. Since the average presentation time of each of the previously used stimuli was 17 seconds, this enabled us to compare the results from all experiments.

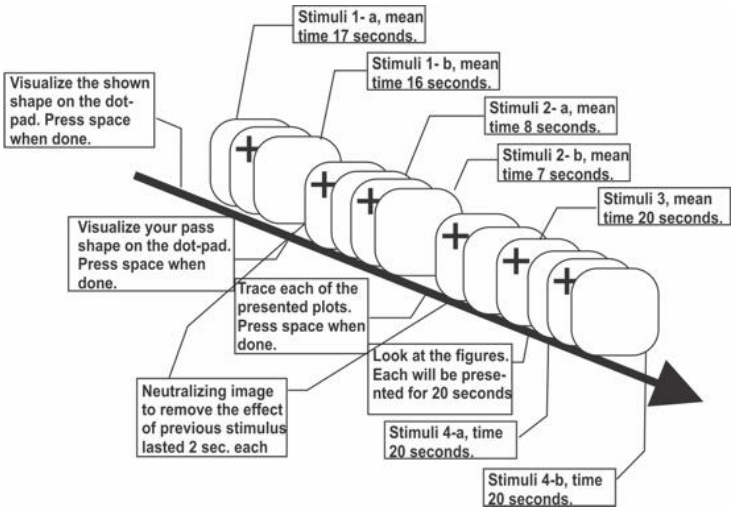

Figure 25. Experiment time sequence, and the order of the presented stimuli.

Fig. 25 summarizes the timeline of the experiments and shows their mean duration. The participants undertook all four experiments sequentially. In Experiment 1, they were presented with the stimulus shown in Fig. 21-a, which was followed by a stimulus that had a cross shape at the screen center, called neutralizing stimulus, which was displayed for 2 seconds. Using the neutralizing stimulus between all displayed stimuli was necessary to re-center the eyes of the participants on the eye tracker display. The stimulus shown in Fig. 21-b was displayed after the neutralizing stimulus. The mean displaying duration of the first and second stimuli was 34 seconds. Experiment 2 displayed the stimuli shown in Fig. 22-a and b, respectively. The mean duration of displaying the stimuli was 16 seconds. Experiment 3 displayed the stimulus shown in Fig. 23; the mean time was 20 seconds. Experiment 4 displayed the stimuli shown in 24-a and b respectively; each image stimulus was displayed for 20 seconds.

3.6 Raw data pre-processing

The eye tracker that we used in the experiments had a frequency of 120 Hz and recorded the actual position of the eye and the physical size of the pupil. The tracker provided an eye movement signal that was noisy; therefore, a pre-processing step was required to remove the noise before we could transform the signal into features. It is important to recognize the source of noise to determine the appropriate filtering method to use. In our case, the noise was caused by *technical* and *human* factors: the technical source of the noise originated from electromagnetic and light interference in the laboratory, whereas the human factor consisted of the eye blinks and head movements of the participants during the eye tracking experiment. In this thesis, we used a low-pass filter and a moving average technique to filter the noise caused by the technical factors and interpolation to recover the lost or badly acquired samples due to human factors.

In this section, the approach of the pre-processing step to filter the eye movement signal is presented. Fig. 26 summarizes the steps that are described hereafter.

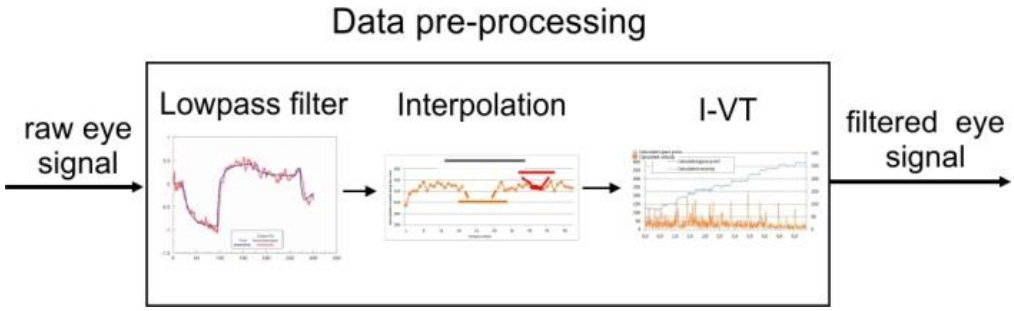

Figure 26. Methodology diagram of data processing (step2).

3.6.1 Noise reduction

The low-pass filter smooth out and reduces the noise spikes of a signal by removing its high frequencies; therefore we chose this filter to process our raw signal. An example of a processed signal with a low-pass filter is illustrated in Fig. 27.

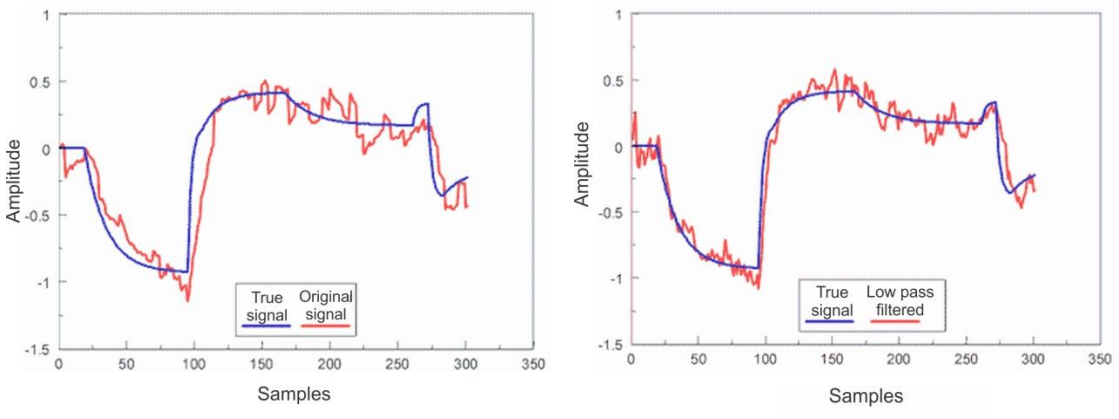

Figure 27. Comparison between a noisy signal and its true signal before filtering (left) and after filtering (right).

The Tobii Software Development Kit (SDK) was used to remove the noise in the signal using a low-pass filter [61]. Then, the non-weighted moving-average filter [67] was applied to provide a further noise reduction to the residual noise in the signal. In this work, we defined the value of the averaging window size to $N = 3$ samples, which means that each sample in the signal is the average of the previous three and next three samples, as given by Eq. 1, where $G[n]$ is the filtered signal and n represents the number of samples in the signal.

$$G[n] = \frac{1}{2*N+1} \sum_{k=-N}^{N} Q[n-k] \qquad \text{Eq. 1}$$

The value of the averaging window has a profound impact on the velocity threshold (I-VT) that is discussed in section 3.6. This is because if the window size is configured to average fewer samples, the I-VT algorithm will identify the quick changes between samples as saccades. On the other hand, if it is configured with a high value to average more samples, the calculated velocity during saccades will be shorter, which may completely discard short fixations. We chose an averaging window size of 3 samples after experimentally testing three values: 3, 5, and 7. We found that taking 5 and 7 samples makes the signal very smooth, causing misidentification errors of the saccades.

There were situations when the previous samples were not found (i.e., the beginning of the signal) and other situations when the later samples were not found (i.e., the end of the signal), which caused the moving average method to be unsuccessful in reducing the noise at the boundaries of the signal. To overcome this situation, we included a threshold value of 25ms at the beginning and end of each experiment before we started processing the signal. This threshold value ensured that there were three samples before the first averaged sample, and three samples after the last averaged sample to provide a moving average with an adequate number of samples at the boundaries.

3.6.2 Normalization and interpolation of the signal

Interpolation is required to fill in the missing samples in the signal. In this work, the interpolation of the eye movement signal is correlated with the identification of fixations and saccades by the I-VT algorithm, and thus requires careful implementation. The missing data can be caused by several factors as explained earlier, and a "filling-the-gaps" procedure must be able to distinguish between those two sources. The following sections describe the interpolation process and the identification of fixations and saccades.

Sample normalization

The eye tracker provided a quality measure (validity code) that is between 1 and 4 for each acquired sample. The value of 0 meant that a high accuracy of the eye position was obtained, and a value of 4 meant that a low accuracy or no sample was recorded. The validity codes are described in Table 3.

The samples that had a value of 2 or 4 in the left and right eyes were discarded as they were poorly recorded by the eye tracker.

Table 3. Validity codes for the Tobii eye-tracker.

Left eye	*Right eye*	*Eyes detected*	*Eye identification*
0	0	Both	Correctly identified
4	0	Right	Correctly identified
0	4	Left	Correctly identified
3	1	Right	Estimated as probable
1	3	Left	Estimated as probable
2	2	One eye	Uncertain
4	4	None	Uncertain

Identifying and interpolating gaps

Gaps caused by the blinks are small and can be interpolated, whereas gaps caused by the eye tracking errors are large and must be discarded. A max-gap-length window was defined to distinguish between the two gaps. The gaps caused by the blinks had a window size of 75 ms [68], and the gaps caused by the temporal obstacle or head movements had more than a 75 ms window size. We used the interpolation method that was proposed by Olsen [69] as given by Eq. 2, where s is a scaling factor and t_{target} is the time stamp of the sample to be interpolated.

$$s = \frac{t_{target} - t_{target+1}}{t_{target-1} - t_{target+1}} \qquad \text{Eq. 2}$$

Interpolating the small gaps replaced the missing samples with approximated ones, which might lower the quality of the signal that we obtained. However, this effect is expected to be marginal because of the limited number of small gaps. An example of the interpolated and discarded gaps is illustrated in Fig. 28. The gap fill-in interpolation was performed for the data collected from each eye separately.

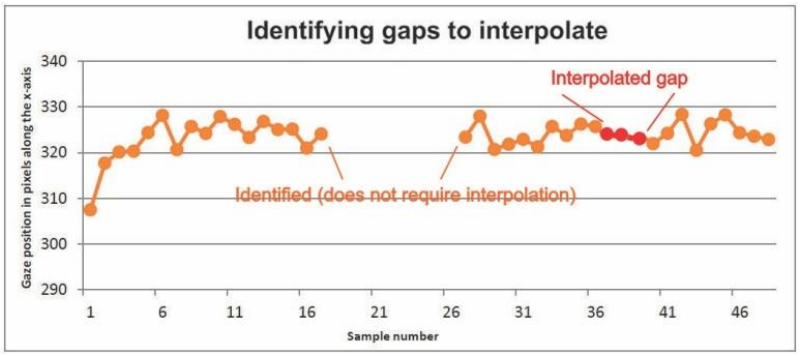

Figure 28. Identifying and interpolating the gaps.

3.7 Extraction of features

After filtering and interpolating the raw signal, the basic dynamic features of the eyes were extracted from the filtered signal. The features included the position of the left and right eyes on the *X* access, and the position of the left and right eyes on the *Y* access. The pupil diameter was also provided by the eye tracker for the left and right eyes. Our method for extracting the features required the identification of the saccades and fixations of the eye movements and the implementation of a statistical procedure. This section provides the method used for extracting the features that were investigated in the work. Fig. 29 shows a sample of the signal that was processed in this section.

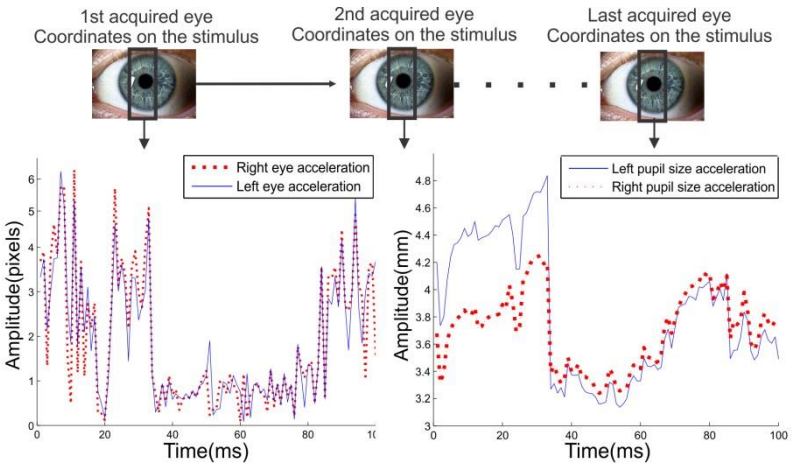

Figure 29. Eye coordinates and pupil size.

3.7.1 Detection of saccades and fixations

The velocity threshold (I-VT) algorithm is a simple fixation identification technique that calculates the velocity of the eyes and identifies the fixations based on a predefined threshold value [25]. I-VT uses the coordinates of the eyes to identify the fixations and saccades in the eye movements; by identifying the eye movement samples that are below the threshold and reporting them as fixations. In this work, we applied a threshold value of 40 °/s based on the recommendation from the work of T. Sen and T. Megaw [70]. The number of fixations and saccades identified by the threshold algorithm varied in the four experiments. Table 4 shows the mean count of saccades and fixations that were calculated by I-VT and the average duration for each experiment.

Table 4. Average time for each experiment and mean count of fixations and saccades.

experiment	*mean count of saccades*	*mean count of fixations*	*average time*
1	11	20	33 seconds
2	7	12	15 seconds
3	9	16	20 seconds
4	15	24	40 seconds

3.7.2 Creating the features of fixations and saccades

The identified fixations and saccades of the eye movements were statistically processed to calculate their acceleration, velocity, and peak values, as elaborated in the next sections.

Variations in pupil size were also investigated during each of the eye's fixation and saccade. Matching was performed by comparing the time stamps provided by the eye tracker for eye movement samples with the time stamps for the pupil size. Fig. 30 illustrates an example of the saccades and fixations of the obtained eye movements and pupil size.

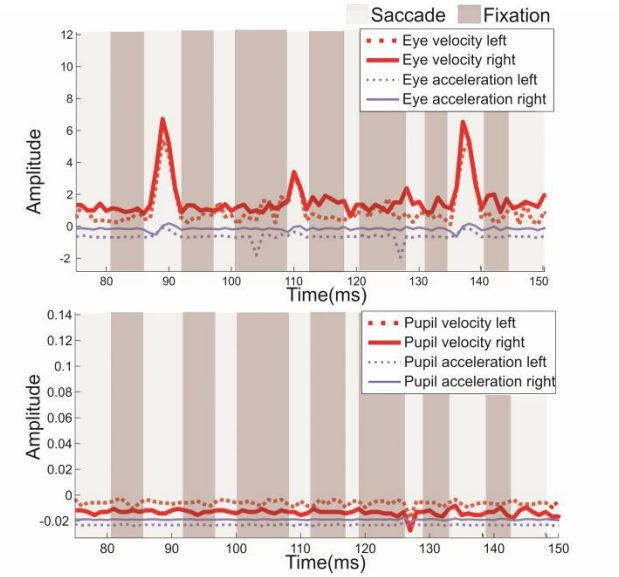

Figure 30. Eye coordinates and pupil size.

3.7.3 Velocity and acceleration of eye movements

The velocity was calculated for the fixations and saccades using the position of the eye at point P_n and point P_{n+1}. The displacement of P_n to P_{n+1} is given by Eq. 3. Fig. 31 shows an illustration of how the movement velocity is derived.

$$\Delta r = \sqrt{(\Delta X)^2 + (\Delta Y)^2} \qquad \text{Eq. 3}$$

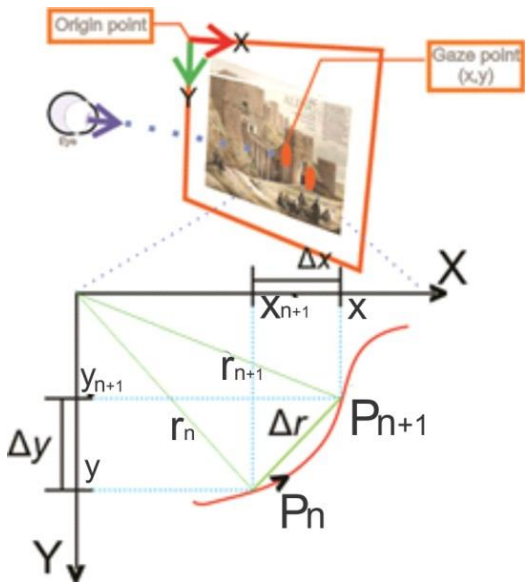

Figure 31. Displacement of eye position Δr between two points $\mathbf{P_n}$ and $\mathbf{P_{n+1}}$.

Taking that Δt is the time interval between P_n and P_{n+1} when the eye moves along a curved path, the average velocity is the ratio of this displacement as given by Eq. 4.

$$\mathcal{V} = \frac{\Delta r}{\Delta t} \qquad \text{Eq. 4}$$

Regardless of the shape of the eye path, its magnitude Δr is always a straight line distance from P_n to P_{n+1}. Thus the eye trackers with a higher refresh rate provide more accurate information about the displacement of the eye. For example, a refresh rate of 120 Hz will yield Δt of 8.33 ms, whereas an eye tracker with higher refresh rate, for example 500 Hz, will yield a Δt of 2 ms. Based on the velocity, the acceleration of the eye movements were obtained from the acceleration function that is given by Eq. 5.

$$\varphi = \frac{\Delta \mathcal{V}}{\Delta t} \qquad \text{Eq. 5}$$

3.7.4 Velocity and acceleration of pupil dilation

The velocity of the pupil size dilation and constriction was found by measuring the differences in pupil diameter by using Eq. 6, where δ is the pupil diameter.

$$\vartheta = \frac{\Delta \delta}{\Delta t} \qquad \text{Eq. 6}$$

The acceleration of pupil dilation and constriction was found by measuring the differences in the velocity of pupil dilation by using Eq. 7.

$$\alpha = \frac{\Delta \vartheta}{\Delta t} \qquad \text{Eq. 7}$$

3.7.5 Distance between eyes

The distance between the eyes (gaze points) is a static biometric trait that was investigated in the work of Kasprowski [46]. We used this trait to increase the classification accuracy of our model as elaborated in Section 4.5. This trait was calculated using the Euclidian distance formula in Eq. 8, where $X_{R,n}$ is the X

coordinate of the *n*th gaze point of the right eye, $X_{L,n}$ is the *X* coordinate of the *n*th gaze point of the left eye, $Y_{R,n}$ is the *Y* coordinate of the *n*th gaze point of the right eye, and $Y_{L,n}$ is the *Y* coordinate of the *n*th gaze point of the left eye.

$$D_n = \sqrt{(X_{R,n} - X_{L,n})^2 + (Y_{R,n} - Y_{L,n})^2} \quad \text{Eq. 8}$$

3.8 Eye movement and iris feature processing

The extracted features from the previous section were processed using Principal Component Analysis (PCA) and the Chi-squared test to select the most relevant features that made up the input vectors for the classification process, as elaborated in the coming sections. The methodology diagram in Fig. 32 summarizes the steps discussed in this section.

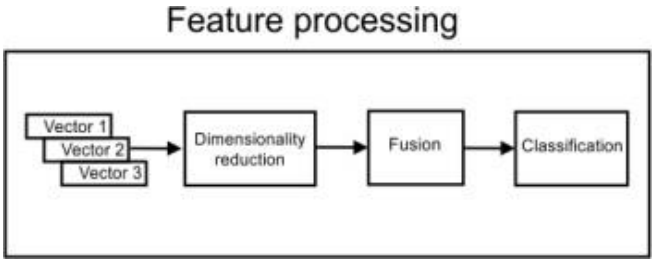

Figure 32. Methodology diagram of feature processing (step3).

3.8.1 Creating vectors

A vector of features was created for each participant in each experiment and was labeled to identify the person that provided the features. A vector was created for each trait, that includes 36 eye movement features, 48 iris features, and 2 features for the distance between the eyes. Table 5 shows the extracted features where μ denotes the feature mean value, σ is its standard deviation, ρ is the peak value, F denotes a fixation and S a saccade, Γ is the difference between the statistical values that were obtained from the left and right eyes, R is right eye, and L is left eye.

Table 5. Features used in this work.

Source	*Type*	*Features*
eye-movements	fixation (*F*)	θ_F^{μ} , θ_F^{σ} , $\mathcal{V}_{F,L}^{\mu}$, $\mathcal{V}_{F,L}^{\sigma}$, $\varphi_{F,L}^{\mu}$, $\varphi_{F,L}^{\sigma}$, $\mathcal{V}_{F,R}^{\mu}$, $\mathcal{V}_{F,R}^{\sigma}$, $\varphi_{F,R}^{\mu}$, $\varphi_{F,R}^{\sigma}$, $\mathcal{V}_{F,L}^{\rho}$, $\varphi_{F,L}^{\rho}$, $\mathcal{V}_{F,R}^{\rho}$, $\varphi_{F,R}^{\rho}$, $\mathcal{V}_{F,\Gamma}^{\mu}$, $\mathcal{V}_{F,\Gamma}^{\sigma}$, $\varphi_{F,\Gamma}^{\mu}$, $\varphi_{F,\Gamma}^{\sigma}$
	saccade (S)	θ_S^{μ} , $\theta_{S_J}^{\sigma}$, $\mathcal{V}_{S,L}^{\mu}$, $\mathcal{V}_{S,L}^{\sigma}$, $\varphi_{S,L}^{\mu}$, $\varphi_{S,L}^{\sigma}$, $\mathcal{V}_{S,R}^{\mu}$, $\mathcal{V}_{S,R}^{\sigma}$, $\varphi_{S,R}^{\mu}$, $\varphi_{S,R}^{\sigma}$, $\mathcal{V}_{S,L}^{\rho}$, $\varphi_{S,L}^{\rho}$, $\mathcal{V}_{S,R}^{\rho}$, $\varphi_{S,R}^{\rho}$, $\mathcal{V}_{S,\Gamma}^{\mu}$, $\mathcal{V}_{S,\Gamma}^{\sigma}$, $\varphi_{S,\Gamma}^{\mu}$, $\varphi_{S,\Gamma}^{\sigma}$
pupil	fixation (*F*)	$\delta_{F,L}^{\mu}$, $\delta_{F,L}^{\sigma}$, $\delta_{F,R}^{\mu}$, $\delta_{F,R}^{\sigma}$, $\vartheta_{F,L}^{\mu}$, $\vartheta_{F,L}^{\sigma}$, $\alpha_{F,L}^{\mu}$, $\alpha_{F,L}^{\sigma}$, $\vartheta_{F,L}^{\rho}$, $\alpha_{F,L}^{\rho}$, $\vartheta_{F,R}^{\mu}$, $\vartheta_{F,R}^{\sigma}$, $\alpha_{F,R}^{\mu}$, $\alpha_{F,R}^{\sigma}$, $\vartheta_{F,R}^{\rho}$, $\alpha_{F,R}^{\rho}$, $\vartheta_{F,\Gamma}^{\mu}$, $\vartheta_{F,\Gamma}^{\sigma}$, $\alpha_{F,\Gamma}^{\mu}$, $\alpha_{F,\Gamma}^{\sigma}$, $\delta_{F,R}^{\mu}$, $\delta_{F,R}^{\sigma}$, $\vartheta_{F,\Gamma}^{\rho}$, $\alpha_{F,\Gamma}^{\rho}$
	saccade (*S*)	$\delta_{S,L}^{\mu}$, $\delta_{S,L}^{\sigma}$, $\delta_{S,R}^{\mu}$, $\delta_{S,R}^{\sigma}$, $\vartheta_{S,L}^{\mu}$, $\vartheta_{S,L}^{\sigma}$, $\alpha_{S,L}^{\mu}$, $\alpha_{S,L}^{\sigma}$, $\vartheta_{S,L}^{\rho}$, $\alpha_{S,L}^{\rho}$, $\vartheta_{S,R}^{\mu}$, $\vartheta_{S,R}^{\sigma}$, $\alpha_{S,R}^{\mu}$, $\alpha_{S,R}^{\sigma}$, $\vartheta_{S,R}^{\rho}$, $\alpha_{S,R}^{\rho}$, $\vartheta_{S,\Gamma}^{\mu}$, $\vartheta_{S,\Gamma}^{\sigma}$, $\alpha_{S,\Gamma}^{\mu}$, $\alpha_{S,\Gamma}^{\sigma}$, $\delta_{S,R}^{\mu}$, $\delta_{S,R}^{\sigma}$, $\vartheta_{S,\Gamma}^{\rho}$, $\alpha_{S,\Gamma}^{\rho}$
distance between eyes (*D*)	fixation (*F*)	$D_{F,\Gamma}$
	saccade (*S*)	$D_{S,\Gamma}$

3.8.1 Normalizing data

The eye movements and iris data were of variable size and scale; therefore it was essential to scale the data variables so that they were comparable. Normalization is a technique that scales each data attribute into a range from 0 to 1 to avoid giving more importance to attributes with larger values. Normalization is given in Eq. 9, where $||x_j||$ is the normalized value of the target feature x_j.

$$||x_j|| = \frac{x_j - x_j^{min}}{x_j^{max} - x_j^{min}} \qquad \text{Eq. 9}$$

3.8.2 Reducing data dimensionality

Some of the extracted features turned out to be completely irrelevant and would thus increase the classification errors. In order to identify and discard such irrelevant features, we used two methods: Principal Component Analysis (PCA) and

Pearson's Chi-squared test. PCA was chosen because it is a widely used method for data processing and dimensionality reduction. For example, it has been used in the area of human face recognition [71] and in gene expression data analysis [72], and has also been investigated for eye movement biometrics [44]. Pearson's Chi-squared test was chosen because of its relatively low overhead computation and ability to rank the relevance of the features to the classification of the model.

PCA transforms the features into a linear combination of all the original variables that contains a relevance description of the original data. The key to the transformation is to produce a set of fewer variables that are linearly-uncorrelated, which is done by finding the eigenvectors and eigenvalues of a features covariance matrix [73]. Let $\sum$ be a matrix for *j* features by *p* variables, and the covariance matrix be ∂. The linear combination of all variables is given by Eq. 10, where the *i* th variable is represented by x_i, and the linear combination coefficients for B_1 is l_{1i}, where i $= 1, 2, \ldots, p$ and is denoted by l_1 , and normalized by $l_1^T l_1$ = 1. The variance of B_1 (first principal component) is given by $l_1^T \partial_{a_1}$ where we can find vector l_1 by maximizing the variance.

$$B_1 = \sum_{i=1}^{p} l_{1i} x_i \qquad \text{Eq. 10}$$

The second principal component that is orthogonal to the first one can be found in a similar manner by maximizing $l_2^T \partial l_1$ which is subject to the constraints $l_2^T l_2$ = 1 and $l_2^T l_1$ = 0. Remaining principal components are derived in a similar way.

The Pearson's Chi-squared test is a statistical technique for computing the relevance of each feature x with respect to class C that it represents. It is a commonly used technique for text classification [74]. The relevance is computer as per Eq. 11, where O_{ij} is the observed frequency and E_{ij} the expected frequency.

$$x^2 = \frac{\sum_{ij}(O_{ij} - E_{ij})^2}{E_{ij}} \qquad \text{Eq. 11}$$

3.8.3 Combining feature vectors

Data fusion was performed to determine whether combining the eye movement features with the iris features in one feature vector reduces the error rate of

the biometric system that we are proposing. Data fusion is a process of combining various sets of data to create a representational data set or decision. In this work, we used feature fusion because it is a widely implemented method in the area of biometrics, and can be carried out on dependent an independent sources of data [75] [76]. For example, feature fusion was implemented by Lupu and Emerich [77] and Ben-Yacoub et al. [78]. Fig. 33 shows a summary of the data fusion process.

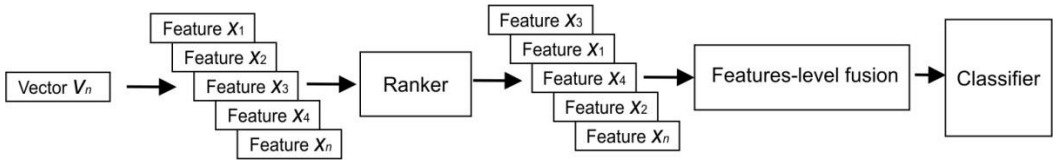

Figure 33. Data fusion diagram.

Combining data was done by using an SVM classifier to evaluate the features in order to rank them based on the relevance in order to improve the prediction of the used classifier. SVM ranks the features by assigning a square value of the attribute weight for each class using a one-vs.-all method [79]. Based on the ranking results, we placed the features in a decreasing order starting at best performance features. Section 5.1.4 provides detailed results of the classification of the combined data and its contribution to our work.

3.9 Classification of features

This section describes the classification approach while the next section evaluates the results. Both steps are illustrated in Figure 34.

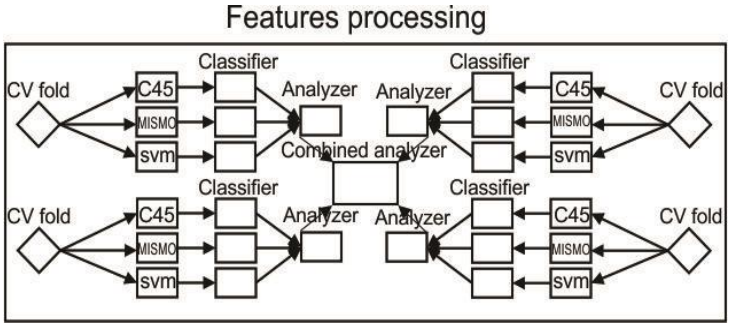

Figure 34. Feature processing and classification for identifying the users based on the collected features (step 4).

Feature classification is a part of the machine learning model that we applied using the Weka data mining package [80]. There are many classification techniques that can be implemented to classify the biometric features in this work. However, based on the past work in eye movement biometrics, we validated our model using C4.5 decision trees, SVM, and Random Forest classifiers. The advantages of using these methods are elaborated in the coming sections and later when analysing the results, and a comparison between the three classifiers is presented to determine which was the best in terms of the accuracy and error rate, as shown in Fig. 37.

3.9.1 Cross-validation

A hold-out method was used to split data into a training set and a test set, which reserves a certain amount of data for validating the classifier later on while the rest is used exclusively for training. To ensure that the results are representative, and to avoid any bias or over-fitting, we repeated this process 10 times, thus deploying 10-fold cross-validation, where the test set comprises 1/10 of the data while the training set consists of the remaining 9/10. This method was applied to all classification techniques as discussed in the following sections.

This technique was used to test our proposed model, therefore when actually implementing the biometric system, the users who are going to be authenticated must provide training samples, which means they must conduct the same experiments as

the other users. The classifier will then be trained anew with the additional data and can subsequently be used to check the user identity.

3.9.2 C45 decision tree

C45 is a decision tree-based algorithm that provides a powerful tool for data classification [83]. We chose this algorithm to classify our data because it has been previously investigated in eye movement biometrics [44], thus making it possible to compare our classification results with results obtained in the literature. C45 finds the most convenient splits from the data sets to describe the class such that the gain is the maximum, and ranks the features based on their relevance to predict the class. The class is computed using the calculated entropy value. The entropy, which is also known as the information value, is the measure of uncertainty of an outcome and is computed by Eq. 12, where p_1, p_2 ,…, p_j of the entropy formula are expressed as fractions that add up to 1.

$$\text{entropy}\ (\boldsymbol{p_1}, \boldsymbol{p_2}\ ,\ldots,\ \boldsymbol{p_j}\ ) = -\ \boldsymbol{p_1}\ \log\ \boldsymbol{p_1} - \boldsymbol{p_2}\ \log\ \boldsymbol{p_2} \ldots - \boldsymbol{p_j}\ \ \log\ \boldsymbol{p_j} \qquad \text{Eq. 12}$$

Splits divide data sets into two subsets and the entropy of both subsets is computed by finding the entropy of the data sets after the split. After computing the gain value, a split is chosen based on the highest gain value and the data set is divided into two tree nodes. The same procedures continue iteratively until a full decision tree is built.

3.9.3 Support Vector Machines

A Support Vector Machine (SVM) is a binary classifier which models the decision boundary between the classes as a separating hyper-plane. It has wide applications in pattern recognition and data classification and has been effectively implemented for eye movement biometrics [44][46]. SVM is considered a robust classifier because it is one of the machine learning techniques that provide a good sample generalization [84], which means that it is capable of choosing an appropriate generalization for the classes even when some bias exists for some features, therefore SVM was used as a data classification technique in this work. Therefore, SVM categorizes the target class as (+1) and the other irrelevant classes as (-1) [85]. Using the categorized training vectors, SVM solves optimization problems and finds a

splitting hyper-plane that maximizes the margin of split between the classes using Eq. 13, where $\alpha_i$is the Lagrangian multiplier which is the weight of each sample from the training set and is found by Eq. 14. C is the target class and v is the features vector.

$$f(x) = sgn(\sum_i \alpha_i C_i \langle v_i, v \rangle) \quad \text{Eq. 13}$$

$$\sum_i \alpha_i - \sum_{ij} \alpha_i \alpha_j C_i C_j \langle v_i, v \rangle \qquad \sum_i \alpha_i = 0, \alpha_i \geq 0 \quad \text{Eq. 14}$$

John Platt's sequential minimal optimization (SMO) algorithm was used for training the support vector classifier [86], because it has been used in biometrics [87]. This version of SVM is not probabilistic, and only a single optimal value of the distance between the separating hyper-plane and origin is obtained for classification. Our employment of SVM using the Weka data mining package [80] used a special modification, which takes a probabilistic approach by assigning a probability value to each prediction using logistic models. We also configured SVM in Weka to use the quadratic Poly-kernel, to consider the interaction of features corresponding to different eye movement and pupil dilation values. In contrast, the original SVM implementation uses a linear Poly-kernel.

The next section discusses the results and findings of the experiments and presents the data classification accuracy and classification errors.

3.9.4 Random Forest classifier

"Random Forest" is an algorithm that is based on the development of many decision tree classifiers [81]. Its main strength is the ability to classify big data sets and handle a large number of variables in a reasonable computing time. It is also capable of handling unbalanced data, as normally occurs when different biometric traits are used, which makes it a good technique to investigate for our data sets. Random Forest applies majority voting to an ensemble of decision trees to improve the classification results [81]. Based on recommendations by Larivière and Poel [82], we experimentally optimized the number of trees to 270 by testing different configurations and selecting that with the highest accuracy.

The Random Forest method is based on generating an ensemble of classification trees known as forests based on a random sampling of features.

Generating forests is essential for passing instances through a voting process to determine the best classification results (often generated by one or more of the trees). Typically, a 10-fold cross-validation is applied by other classifiers to avoid bias in splitting data into training and testing sets.

4 Experimental Results

This section presents the outcomes of the experiments and the classification results of the features that were extracted. An evaluation of the outcomes is provided to hypothesize which method was the most viable for building a biometric identification system.

4.1 Ranking features

The classification process was carried out on the most relevant features as described herein. For simplicity, only 10 relevant and irrelevant features are shown in Fig. 35. A full description of the notations is provided in Appendix A.

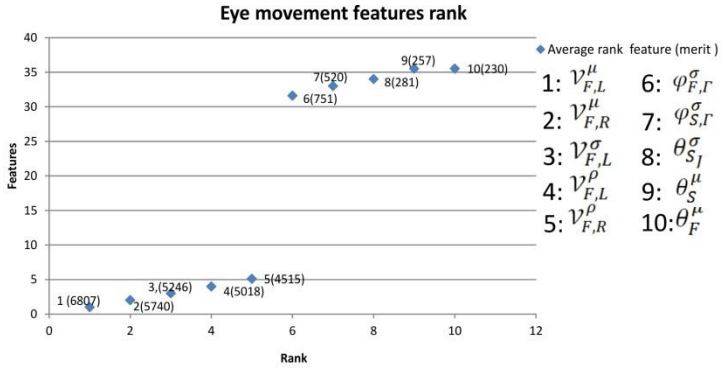

Figure 35. Ranked attributes obtained from a Chi-squared test for eye movement features. 1 indicates the highest rank and 10 indicates the lowest rank.

The lowest ranked features shown in Fig. 35 were removed in addition to 7 more features that were ranked as irrelevant features. These included: $\varphi^{\mu}_{S,\Gamma}$, $\varphi^{\mu}_{F,\Gamma}$, θ^{μ}_{S} , $\mathcal{V}^{\mu}_{F,\Gamma}$, $\varphi^{\sigma}_{S,R}$, $\varphi^{\sigma}_{S,L}$, and $\varphi^{\sigma}_{F,\Gamma}$. We determined the irrelevant features heuristically, by removing the feature that ranked the worst and running the classifier using the remaining features. We repeated this process until the accuracy obtained was less than the previous one.

A similar technique was followed to remove the irrelevant pupil features which included: $\alpha^{\mu}_{F,L}$, $\alpha^{\sigma}_{F,L}$, $\vartheta^{\rho}_{F,L}$, $\alpha^{\rho}_{F,L}$, $\vartheta^{\mu}_{F,R}$, $\vartheta^{\sigma}_{F,R}$, $\alpha^{\mu}_{F,R}$, $\vartheta^{\sigma}_{F,\Gamma}$, $\alpha^{\mu}_{F,\Gamma}$, $\alpha^{\sigma}_{F,\Gamma}$, $\vartheta^{\sigma}_{S,R}$, $\alpha^{\mu}_{S,R}$, $\alpha^{\sigma}_{S,R}$, $\vartheta^{\rho}_{S,R}$, $\alpha^{\rho}_{S,R}$.

The lowest ranked features that were removed after combining eye movement and iris features included: $\varphi_{F,R}^{\rho}$, $\mathcal{V}_{F,\Gamma}^{\mu}$, $\mathcal{V}_{F,\Gamma}^{\sigma}$, $\varphi_{F,\Gamma}^{\mu}$, $\mathcal{V}_{S,L}^{\sigma}$, $\varphi_{S,L}^{\mu}$, $\varphi_{S,L}^{\sigma}$, $\mathcal{V}_{S,R}^{\mu}$, $\mathcal{V}_{S,R}^{\sigma}$, $\vartheta_{F,L}^{\mu}$, $\vartheta_{F,L}^{\sigma}$, $\alpha_{F,L}^{\mu}$, $\alpha_{F,L}^{\sigma}$, $\vartheta_{F,L}^{\rho}$, $\alpha_{F,L}^{\rho}$, $\vartheta_{F,R}^{\mu}$, $\alpha_{S,R}^{\rho}$, $\vartheta_{S,\Gamma}^{\mu}$, $\vartheta_{S,\Gamma}^{\sigma}$, $\alpha_{S,\Gamma}^{\mu}$, $\alpha_{S,\Gamma}^{\sigma}$, $\delta_{F,L}^{\mu}$, $\delta_{F,L}^{\sigma}$, $\delta_{F,R}^{\mu}$, $\delta_{F,R}^{\sigma}$. Table 6 summarizes the number of features initially defined, removed via ranking, and used for classification purposes, respectively.

Table 6. Number of features defined, removed, and used in the classification.

Source of features	*Defined initially*	*Removed*	*Used*
Eye movements	36	12	24
Iris	48	30	18
Distance between the eyes	2	0	2

4.2 Eye movement classification

The percent of correctly-classified instances of data obtained from the 17 participants using SVM was 35% for Experiment 1. The mean performance metrics of Experiment 1 are shown in Table 7 with the other three Experiments. The total percentage of correctly classified instances in Experiment 2, 3, and 4 was lower and reached as low as 31% of correctly-classified instances.

The classification accuracy of C45 was also low, especially when compared with the other investigated classifiers in this work. C45 correctly classified 32% of the instances in Experiment 1. The classification accuracy was improved for Experiment 2 and yielded 35% of correctly classified instances. It was also lower in Experiment 4 where the correctly classified instances were 24%.

Experiment 1 had 44% of correctly classified instances, which was higher than the obtained accuracy from the C45 and SVM classifiers. The lowest classification accuracy was obtained from Experiment 4, where the correctly identified instances were 37%.

Table 7. Accuracy and error rate results obtained from classifying eye movement data.

Classifier		*FAR*	*FRR*	*HTER*	*Precision*	*Recall*
SVM	Exp1	0.051	0.647	0.349	0.356	0.353
	Exp2	0.044	0.648	**0.346**	0.351	0.352
	Exp3	0.049	0.676	0.3625	0.309	0.324
	Exp4	0.05	0.702	0.376	0.295	0.298
	Combined	0.047	0.673	0.36	0.322	0.327
C45	Exp1	0.06	0.681	0.3705	0.302	0.319
	Exp2	0.046	0.647	**0.3465**	0.343	0.353
	Exp3	0.048	0.705	0.3765	0.301	0.295
	Exp4	0.054	0.761	0.4075	0.239	0.239
	Combined	0.052	0.763	0.4075	0.239	0.237
Random forest	Exp1	0.056	0.557	**0.3065**	0.431	0.443
	Exp2	0.045	0.574	0.3095	0.409	0.426
	Exp3	0.046	0.574	0.31	0.41	0.426
	Exp4	0.046	0.623	0.3345	0.369	0.377
	Combined	0.047	0.638	0.3425	0.347	0.362

The results suggest that the biometric identification using eye movements alone provide high error rate. This is because the stimuli that were presented in Experiments 1–3 provided an average HTER of 31%, and the stimuli that were presented in Experiment 4 provided an HTER of 33%. The results also show a small difference in the error rate obtained across all experiments, where the maximum difference was only 3%. Combining the data from all experiments also produced a high error rate as shown in Table 7.

The main conclusions to be drawn from these results are: (1) the eye movement features that were investigated in this work achieved an error rate relatively higher than the error rate attained by Kasprowski and Ober [44], Komogortsev et al. [40], Kinnunen et al. [41], and Rigas et al. [50]. However, in this work we used a much simpler stimuli that could serve as a general-purpose methods for stimulating eye movements; (2) the influence of the stimulus on the eye movements was marginal because all experiments yielded almost similar HTERs, with a mean of 32% and a standard deviation of 1.6%.

4.3 Iris classification

Using SVM to classify iris features yielded better performance and accuracy than that obtained from classifying eye movement features. Experiment 1 yielded

76% correctly-classified instances and Experiment 2 and 3 yielded a similar value. The total number of correctly classified instances for experiment 4 was 62%, and combining data from all Experiments in one classifier yielded 60% correctly-classified instances.

Using the C45 algorithm provided results similar to SVM. Experiment 1 yielded 74% correctly-classified instances and Experiment 2 yielded the highest classification accuracy with 78%. Combining data from the presented four experiments produced a lower accuracy with 58% correctly-classified instances.

As we expected, using Random Forest with 270 trees yielded better accuracy than the previous techniques, and that is because it uses an ensemble method. The highest obtained was in Experiment 1 which yielded 84% correctly-classified instances. Experiments 2 and 3 yielded 86% correctly classified instances; however, Experiment 4 yielded the lowest accuracy with 71% correctly classified instances. When all data extracted from the four experiments were classified in one classifier, they yielded 69% accuracy.

Table 8. Accuracy and error rate results obtained from classifying iris data.

Classifier		*FAR*	*FRR*	*HTER*	*Precision*	*Recall*
SVM	Exp1	0.02	0.237	0.1285	0.751	0.763
	Exp2	0.016	0.231	**0.1235**	0.768	0.769
	Exp3	0.017	0.249	0.133	0.749	0.751
	Exp4	0.027	0.374	0.2005	0.626	0.626
	Combined	0.029	0.399	0.214	0.592	0.601
C45	Exp1	0.021	0.257	0.139	0.739	0.743
	Exp2	0.015	0.214	**0.1145**	0.785	0.786
	Exp3	0.016	0.248	0.132	0.756	0.752
	Exp4	0.028	0.396	0.212	0.607	0.604
	Combined	0.029	0.424	0.2265	0.576	0.576
Random Forest	Exp1	0.015	0.155	**0.085**	0.842	0.845
	Exp2	0.011	0.143	**0.077**	0.858	0.857
	Exp3	0.011	0.155	**0.083**	0.845	0.845
	Exp4	0.02	0.289	0.1545	0.711	0.711
	Combined	0.022	0.3	0.161	0.693	0.698

The results shown in Table 8 suggest that the velocity and acceleration of pupil size variations can provide good biometric accuracy. The Half Total Error Rate (HTER) of 7.7% computed from Experiment 2 appears to be the best, whereas the

worst obtained HTER was 15.4% in Experiment 4. The results also show a lower difference in the error rate obtained across all experiments compared to that attained error rate from eye movements. That is because the difference in the achieved HTER in Experiments 2 and 4 was 7.7%, which is approximately a 100% increase in Experiment 4. This conclusion, however, must be further validated with studies that should include a big sample group of users; our study had only 17 users.

The main conclusions to be drawn from these results are: (1) the pupil features that were investigated in this work achieved a much lower biometric error rate than eye movements; (2) the influence of the stimulus on the iris features was considerable; that is caused by the correlation between the iris constriction and dilation with the cognitive factors [17]. Hence the stimulus is an important factor for obtaining iris features for biometric identification.

4.4 Classification of the combined eye movements and iris data

We used a similar SVM configuration to classify fused eye movements and iris data. The first experiment yielded the highest accuracy with 77% of correctly classified instances; the lowest accuracy was obtained from Experiment 4 where the correctly classified instances were 66%. The combined data sets from all experiments yielded similar accuracy.

The C45 classification tree model had a better classification accuracy. The correctly-classified instances were 81% in Experiment 1, Experiment 4 yielded the lowest accuracy with 67% correctly classified instances. Combining the experiments data set and classifying them using C45 yielded 66% correctly-classified instances.

Classifying the data set with Random Forest improved the classification accuracy. Experiments 1, 2, and 3 yielded approximately 90% correctly-identified instances. However, Experiment 4 and data combined from all experiments yielded lower accuracy with 79% of correctly classified instances.

The results that are shown in Table 9 suggest that a low error rate in biometric identification is achievable using the presented technique. Experiments 1 and 2 attained a promising HTER, which was 5.3%; this value was the best across all conducted experiments. The worst HTER value was 11.4%, which was obtained from Experiment 4. This indicates that the stimuli that require a task to be performed, for

example stimulus 1 and 2, are better-suited for eye dynamic-based biometrics than the image-based stimulus.

Table 9. Accuracy and error rate results obtained from classifying combined eye movements and iris data.

Classifier		*FAR*	*FRR*	*HTER*	*Precision*	*Recall*
SVM	Exp1	0.019	0.231	**0.125**	0.773	0.769
	Exp2	0.021	0.321	0.171	0.687	0.679
	Exp3	0.017	0.25	0.1335	0.757	0.75
	Exp4	0.024	0.337	0.1805	0.662	0.663
	Combined	0.025	0.353	0.189	0.639	0.647
C45	Exp1	0.017	0.129	**0.073**	0.81	0.808
	Exp2	0.012	0.174	0.093	0.829	0.826
	Exp3	0.014	0.214	0.114	0.788	0.786
	Exp4	0.023	0.33	0.1765	0.672	0.67
	Combined	0.023	0.334	0.1785	0.666	0.666
Random Forest	Exp1	0.006	0.1	**0.053**	0.911	0.9
	Exp2	0.007	0.099	**0.053**	0.909	0.901
	Exp3	0.007	0.11	0.0585	0.89	0.89
	Exp4	0.015	0.212	0.1135	0.788	0.788
	Combined	0.016	0.22	0.118	0.777	0.78

The main conclusions to be drawn from these results are:

(1) Fusing eye movements and iris data considerably lowered the error rate of biometric identification using eye movements. The significance of this technique is its leveraging of the dynamic features that were obtained from the eyes.

(2) The low error rate obtained is very promising and a first step towards achieving a commercially usable method for identification and authentication services. However, more validation is required with studies that include a larger sample group of users.

4.5 Classification of the combined eye movement, iris, and distance between eyes

Experiments 1, 2, and 3 yielded 81% correctly-classified instances when the SVM classification algorithm was used. The correctly-classified instances in Experiment 4 were 89%. The combined data set from all experiments yielded 79 % correctly-classified instances.

The classification tree model C45 correctly classified 90% of instances in Experiment 1. Experiment 2 yielded 91% correctly-classified instances. Experiment 3 yielded 88% correctly-classified instances. Both Experiment 4 and combined data yielded 84% correctly-classified instances.

Using Random Forest as a clarification method lowered the error rate like it did in the previous experiments that investigated other features. All experiments yielded very low error rate, as shown in Table 10.

Table 10. Accuracy and error rate results obtained from classifying combined eye movements, iris, and distance between the eyes data.

Classifier		*FAR*	*FRR*	*HTER*	*Precision*	*Recall*
SVM	Exp1	0.010	0.165	0.087	**0.810**	**0.835**
	Exp2	0.013	0.16	0.086	**0.815**	**0.840**
	Exp3	0.019	0.18	0.0995	**0.816**	**0.82**
	Exp4	0.021	0.187	0.104	0.891	0.813
	Combined	0.022	0.195	0.108	0.792	0.805
C45	Exp1	0.009	0.096	0.052	0.907	0.904
	Exp2	0.009	0.1	0.054	0.91	0.9
	Exp3	0.01	0.12	0.065	0.88	0.88
	Exp4	0.011	0.154	0.082	0.845	0.846
	Combined	0.014	0.18	0.097	0.83	0.82
Random Forest	Exp1	0.0001	0.002	0.00105	0.999	0.998
	Exp2	0.0004	0.003	0.0017	0.996	0.997
	Exp3	0.0009	0.01	0.0054	0.99	0.99
	Exp4	0.001	0.01	0.0055	0.99	0.99
	Combined	0.001	0.012	0.0065	0.988	0.988

The results show that combining the distance between the eyes, which is a static biometric feature, with the dynamic features of the eyes achieves the lowest error rate. All experiments achieved a very good HTER, which was between 0.1% and 0.5%. This indicates that using the static features might be beneficial and help lowering the error rate of the biometric system. However, the distance between the eyes might turn out to be not distinctive enough if deployed on a large scale.

5 Discussion and conclusion

5.1 Task-driven vs. task-independent stimuli

Relying on task-independent methods for extracting eye movement features for biometric identification was shown to be possible. Encouraging results were obtained when image-based stimuli were presented (Section 3.5.2 discussed a detailed experimental scenario). Fig. 36 shows a comparison between the task-driven stimuli and task-independent stimuli of the obtained HTER when eye movements and iris data were fused. The task-driven stimuli achieved lower HTER rate with an average HTER of 5.5%, whereas task-independent stimuli achieved an HTER of 11%.

Figure 36. Comparison of the obtained accuracy results from eye movements alone across all experiments.

5.2 Effect of stimuli on eye movements and iris

Interesting results were obtained from comparing Experiments 2 and 4 as illustrated in Fig. 37. Experiment 2 was task-driven and consisted of a task that required long-term cognition, and Experiment 4 was task-independent and consisted of an image-based stimulus. In Experiment 2, the difference between the obtained HTER error rate from eye movements and irises was the highest because eye movements yielded an HTER of 31% and irises yielded 7.7%. This indicates that the stimulus in Experiment 2 was the worst across all task-driven stimuli for eye

movements and best for irises. Further investigation is required on the influence of the cognitive factor on this behavior.

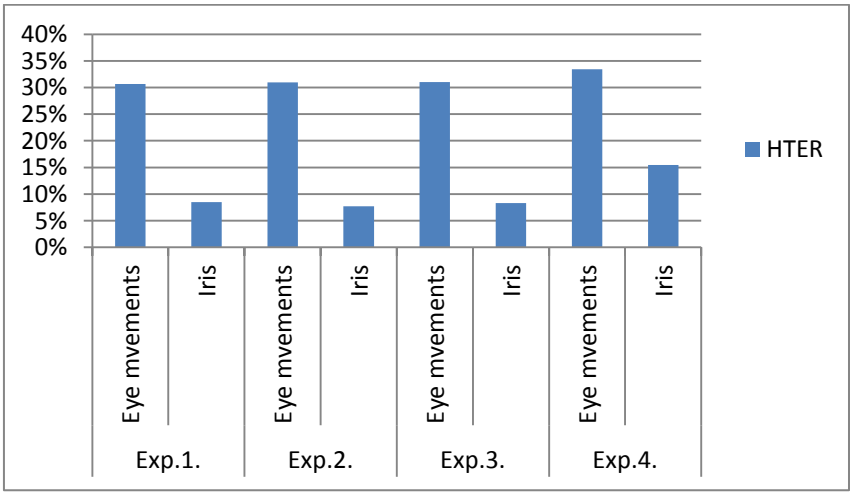

Figure 37. Comparison of the obtained error rates between eye movements and iris across all experiments.

In Experiment 4, the obtained HTER from the iris was almost 94% worse than the other experiments, whereas eye movements in Experiment 4 were only 10% worse than the previous experiments (1, 2, 3, and 4). The main conclusion that can be drawn from this behavior is that the pupil size changes are far more influenced by the stimulus type than eye movements. This behavior could originate from the fact that the size of the pupil is more correlated with the cognitive factor and the difficulty level of the stimulus.

5.3 Effect of using random stimuli

In order to test the viability of using random stimuli for eye movement biometrics, we combined the data sets obtained from the experiments in a single data file and used it for classification. In this case, using cross-validation randomly divided the data sets into training and testing data. The results illustrated in Fig. 38 show an HTER of 10.5%, which is approximately 90% less than the error rate that was obtained by Komogortsev et. al. [42]. The main conclusion that can be reached from these results, as well as the findings in the previous work presented in the literature review, is that it is possible to extract usable data from the eyes to serve as a biometric

trait for biometric identification when most types of stimuli are used to excite the eyes. The error rate of the biometric identification decreases when tasks that require long-term cognition are used.

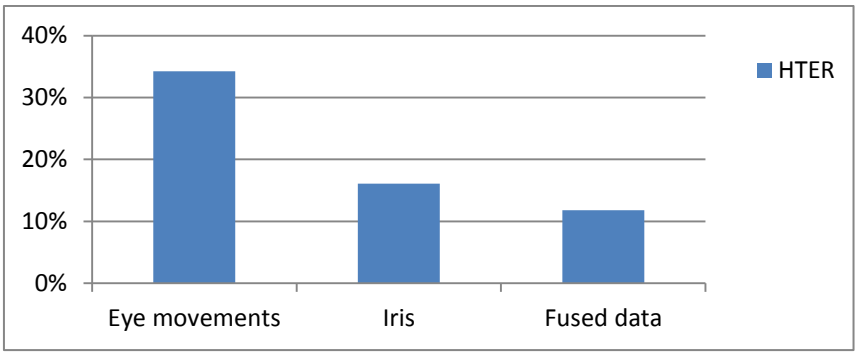

Figure 38. Comparison of the obtained error rates from combined eye movements, irises, and fused eye movements and iris data.

5.4 Achievements

This thesis proposed a task-independent approach designed to extract dynamic features from the eyes for biometric identification. We showed that extracting eye movements for biometric identification using a stimulus other that the one used for training the biometric system is practical, thus making task-independent person recognition possible for many security and general-purpose applications.

The work investigated four different stimuli and compared the Half Total Error Rate (HTER) that was obtained using each stimulus. The results indicated that the stimulus impacts the quality of extracted eye movement features. However, all investigated stimuli were a useful source for obtaining eye movement features for biometrics.

We found that the pupil constriction and dilation behavior is a biometric trait that can achieve far better biometric identification accuracy than eye movements. Therefore we proposed a method to increase the accuracy in eye movement biometrics by incorporating iris features with eye movement features. Our multi-feature model decreased the HTER value from 30% to 5.3%.

We also investigated the distance between the eyes as a biometric trait and combined it with iris and eye movement features. The HTER value that was obtained from this approach was 0.105%. This very low error rate could be sufficient to

propose a commercially-usable eye movements-based biometric system for identification and authentication purposes.

5.5 Limitations

It is worth mentioning that this work and previous work presented in the literature review had a small sample of users. Therefore, hypothesizing to use the dynamic features of the eyes as a biometric trait requires more investigation and testing on a larger group of users. While the small number of participants in this research domain is considered a limitation, the high cost of an eye tracking apparatus is another issue in the future implementation of such biometrics as a general-purpose identification method.

Also, the behavior of the eyes in individuals requires further investigation to hypothesize whether the oculomotor plant that moves the eyes changes it properties in individuals when they age or suffer from ocular diseases.

5.6 Future work

In future work, new eye movement and iris features must be examined, and new feature extraction methods must be investigated such as, the Gaussian mixture model (GMM) and Hidden Markov Model (HMM) which were widely implemented for feature extraction in speech recognition [88][89], in order to improve the accuracy of similar systems. Both GMM and HMM were used in extracting features in the text-independent speaker recognition area [90], which might also be used to extract new features for the task-independent eye movement biometrics. The cognitive factors must also be investigated, such as the impact of task complexity on eye movements in correlation with the stimuli used to excite the eyes and extract their dynamic features, and the influence of using well-known images and the learning effect on eyes dynamics, in order to propose a highly viable stimulus for this kind of biometric identification.

A larger group of users will need to be included in future work to attempt to build a large database of dynamic eye features to test this biometric method on a large scale. The eye tracking experiments must also be conducted in different places such as public and open areas; to test the impact of the environment on the identification

accuracy, and to investigate the efficiency of the proposed system for stealth identification in vital facilities such as airports and public services.

6 References

[1] R. Cappelli, D. Maio, D. Maltoni, J.L. Wayman, A. K. Jain, "Performance evaluation of fingerprint verification systems," *IEEE Transactions on Pattern Analysis and Machine Intelligence*, vol.28, no. 1, pp. 3-18, Jan. 2006.

[2] L. Juwei, K. N. Plataniotis, and A. N. Venetsanopoulos, "Face recognition using LDA-based algorithms," *IEEE Transactions on Neural Networks*, vol. 14, no. 1, pp. 195- 200, Jan. 2003.

[3] S. Weicheng and R. Khanna, "Prolog To Iris Recognition: An Emerging Biometric Technology," in *Proceedings of the IEEE*, vol. 85, no. 9, pp. 13-47, Sept. 1997.

[4] C. Roberts, "Biometric attack vectors and defences," *Computers & Security*, Vol. 26, no. 1, pp. 14-25, Feb. 2007.

[5] S. A. Israel, W. T. Scruggs, W. J. Worek, J. M. Irvine, "Fusing face and ECG for personal identification," in *Proceedings of Applied Imagery Pattern Recognition Workshop*, pp. 226- 231, 2003.

[6] A. Chatterjee, R. Fournier, A. Nait-Ali, P. Siarry, "A Postural Information-Based Biometric Authentication System Employing S-Transform, Radial Basis Function Network, and Extended Kalman Filtering," in *Proceedings of the IEEE Transactions on Instrumentation and Measurement*,vol.59, no.12, pp. 3131-3138, Dec. 2010.

[7] Y. Zhong, Y. Deng, and A. K. Jain, "Keystroke dynamics for user authentication," in *Proceedings of the IEEE Computer Society Conference on Computer Vision and Pattern Recognition Workshops (CVPRW)*, vol.2, no.3, pp.117-123, June 2012.

[8] P. Kasprowski, O. V. Komogortsev, and A. Karpov,"First eye movement verification and identification competition at BTAS 2012," *IEEE Fifth International Conference on Biometrics: Theory, Applications and Systems (BTAS)*, pp. 195-202, 2012.

[9] O. V. Komogortsev, A. Karpov, C. Holland, H. P. Proença, "Multimodal Ocular Biometrics Approach: A Feasibility Study," In *Proceedings of the IEEE Fifth International Conference on Biometrics: Theory, Applications and Systems (BTAS)*, pp. 1-8, 2012.

[10] R. Bednarik, T. Kinnunen, A. Mihaila, P. Fränti, " Eye-movements as a biometric," in *Proceedings of the 14 Scandinavian Conference on Image Analysis*, Lecture Notes in Computer Science, Springer-Verlag, vol. 35, pp. 780-789, 2005.

[11] A. K. Jain and A. Ross. "Introduction to Biometrics". A. *Handbook of Biometrics*. Springer. pp. 1-22, 2008.

[12] A. K. Jain, L. Hong, and S. Pankanti. "Biometric Identification". *Communications of the ACM*, vol. 43, issue 2, pp. 91-98, 2000.

[13] Zephyr Analysis. "International Biometric Group. Internet: www.biometricgroup.com, [March13, 2012].

[14] J. R. Anderson, *Visual attention. In Cognitive Psychology and its Implications*. 4th Edition, W. H. Freeman & Company New York, pp. 81-105, 1995.

[15] A. Rhcastilhos. "Schematic diagram of the human eye." Internet: http://commons.wikimedia.org/wiki/File:Schematic_diagram_of_the_eye_en.svg, Feb. 02, 2008 [Aug. 26, 2012].

[16] H. D. Schubert, "Structure and function of the neural retina" in *Ophthalmology: Expert Consult*, 3rd ed., vol. M. Yanoff, J, Duker, Ed. Mosby, pp. 511-513, 1999.

[17] D. Drieghe, M. Brysbaert, and T. Desmet, "Parafoveal-on-foveal effects on eye movements in text reading: Does an extra space make a difference?" *Vision Research*, vol. 45, issue 13, pp. 1693-1706, June 2005.

[18] K. Rayner, "Eye movements in reading and information processing: 20 years of research." *Psychological Bulletin*, vol. 124, no. 3, pp. 372-422, 1998.

[19] H. Gioanni, J. Rey, J. Villalobos, J.J. Bouyer, Y. Gioanni," Optokinetic nystagmus in the pigeon (Columba livia)." *Experimental Brain Research*, vol. 44, pp. 362–370, Dec. 1981.

[20] Science photolibrary, "Eye muscles." Internet: http://medical-transcriptionist-reference.blogspot.com/2012/05/eye-muscles.html, Jan. 21, 2001[December. 24, 2013].

[21] K. S. Saladin. Anatomy and Physiology. McGraw-Hill, pp. 616–617, 2012.

[22] O. V. Komogortsev, Gobert, V. Denise, V. Jayarathna, K. Sampath, D. Hyong, S. M. Gowda, "Standardization of Automated Analyses of Oculomotor Fixation and Saccadic Behaviors." *IEEE Transactions on Biomedical Engineering*, vol. 57, no. 11, pp. 2635 – 2645, Nov. 2010.

[23] K. Rayner, "Eye movements in reading and information processing: 20 years of research." *Psychological Bulletin*, vol. 124, no. 3, pp. 372-422, 1998.

[24] P. Kasprowski and J. Ober, "Eye movement tracking for human identification," *6th World Conference Biometrics*, pp. 79-112, 2003.

[25] D. D. Salvucci and J. H. Goldberg, "Identifying fixations and saccades in eye-tracking protocols " in *Proceedings of the symposium on Eye tracking research & applications-ETRA '00*, vol. 5, pp. 71-78, 2000.

[26] Tobii Technology. "Tobii T120 Eye Tracker," Internet: http://www.tobii.com/, Dec. 2012 [Jan. 2013].

[27] B. Winn, D. Whitaker, D.B. Elliott, N.J. Phillips, "Factors affecting light-adapted pupil size in normal human subjects," Investigative Ophthalmology and Visual Science, vol. 35, pp. 1132–1137, 1994.

[28] C. Privitera, L. Renninger, T. Carney, S. Klein, M. Aguilar, "Pupil dilation during visual target detection," *Journal of Vison*, vol. 10, pp. 1-10, Aug. 2010.

[29] M. Naber, S. Frässle, and W. Einhäuser, "Perceptual Rivalry: Reflexes Reveal the Gradual Nature of Visual Awareness." *Public Library of Science, PLoS One* ,vol. 6, pp. 910-916, 2011.

[30] A. Muron and J. Pospisil, "The human iris structure and its usages," *Natural Physics*, vol. 39, pp. 87–95, 2000.

[31] L. Cowen, L. J. Ball, and J. Delin, "An eye-movement analysis of web-page usability" in *People and Computers XVI—Memorable Yet Invisible: Proceedings of HCI 2002*, X. Faulkner, J. Finlay, and F. Détienne, Ed. London: Springer-Verlag Ltd, pp. 317-335, 2002.

[32] A. Darwish and E. Bataineh, "Eye tracking analysis of browser security indicators," in *Proceedings of the IEEE International Conference on Computer Systems and Industrial Informatics*, vol.1, pp.18-20, Dec. 2012.

[33] M. Schiessl, S. Duda, A. Thölke, and R. Fischer, "Eye Tracking and Its Application In Usability And Media Research." *MMI-Interaktiv*, vol. 6, no. 6, pp. 1-6, 2003.

[34] A. Borji, "Boosting bottom-up and top-down visual features for saliency estimation," *IEEE Conference on Computer Vision and Pattern Recognition (CVPR)*, pp. 438-445, 2012.

[35] K. Humphrey and G. Underwood, "Eye movements and scanpaths in the perception of real-world scenes." Ph.D. thesis, University of Nottingham, U.K., 2010. D. L. Silver and A. Biggs."Keystroke and Eye-Tracking Biometrics for User Identification" in *Proceedings of IC-AI*, pp. 344-348, 2006.

[36] D. Noton and L. Stark, "Scanpaths in saccadic eye movements while viewing and recognizing patterns", *Vision Research*, vol. 11, Issue 9, pp. 929-942, 1971.

[37] C. Holland, and O. V. Komogortsev, "Biometric identification via eye movement scanpaths in reading," *International Joint Conference on Biometrics (IJCB)*, pp. 1-8, Oct. 2011.

[38] R. Bednarik, T. Kinnunen, A. Mihaila, P. Fränti, " Eye-movements as a biometrics," in *14 Scandinavian Conference on Image Analysis*, Lecture Notes in Computer Science, Springer-Verlag, vol. 3540, pp. 780-789, 2005.

[39] H. Rorschach, *Rorschach Test - Psychodiagnostic Plates*. Hogrefe, pp. 1-10, 1927.

[40] O. V. Komogortsev, S. Jayarathna, C. R. Aragon, M. Mahmoud, "Biometric identification via an oculomotor plant mathematical model," in *Proceedings of the 2010 Symposium on Eye-Tracking Research Applications (ETRA '10)*, pp. 57-60, 2010.

[41] T. Kinnunen, F. Sedlak, and R. Bednarik, "Towards task-independent person authentication using eye movement signals," in *Proceedings of the 2010 Symposium on Eye-Tracking Research Applications (ETRA '10)*. pp. 187-190, 2010.

[42] O. V. Komogortsev, A. Karpov, L. Price, C. Aragon, "Biometric Authentication via Oculomotor Plant Characteristic" in *Proceedings of the IEEE/IARP International Conference on Biometrics (ICB)*, pp. 1-8, 2012.

[43] A. Bulling, J. A. Ward, H. Gellersen, G. Tröster, "Eye Movement Analysis for Activity Recognition Using Electrooculography" *IEEE Transaction on Pattern Analysis and Machine Intelligence*, pp. 741-753, 2011.

[44] P. Kasprowski, and J. Ober, "Eye Movement in Biometrics," *Proceedings of Biometric Authentication Workshop, European Conference on Computer Vision,* pp. 248-258, 2004.

[45] W. J. Donnelly and A. Roorda, "Optimal pupil size in the human eye for axial resolution," *Journal of Optical Society of America*, vol. 11, pp. 2010–2015, 2003.

[46] P. Kasprowski, Human Identification Using Eye Movements, Ph. D. Dissertation. Silesian University of Technology, Gliwice, Poland, 2004.

[47] R. A. Calvo, M. Partridge, and M. A. Jabri, "A Comparative Study of Principal Component Analysis Techniques," in *Proceedings of the Ninth Australian Conference on Neural Networks*, Brisbane, pp.1-25, 1998.

[48] A. Klami, C. Saunders, T. E. de Campos, and S. Kaski, "Can relevance of images be inferred from eye movements?" in *Proceedings of the 1st ACM international conference on Multimedia information retrieval* (MIR '08), pp. 134-140, 2008.

[49] J. You, W. K. Kong, D. Zhang, K. H. Cheung, "On hierarchical palmprint coding with multiple features for personal identification in large databases" *IEEE Transactions on Circuits and Systems for Video Technology*, vol. 14, pp. 234– 243, 2004.

[50] I. Rigas, G. Economou, and S. Fotopoulos, "Biometric Identification Based On The Eye Movements And Graph Matching Techniques", *Pattern Recognition Letters*, vol. 33, issue 6, pp. 786-792, April 2012.

[51] M. Brown, M. Marmor, and V. Vaegan, "ISCEV Standard for Clinical Electro-oculography (EOG)," *Documenta Ophthalmologica*, vol. 113, no. 3, pp. 205–212, 2006.

[52] A. Poole and L. J. Ball, "Eye tracking in Human-Computer interaction and usability research: Current status and future prospects" in *Claude Ghaoui, editor, Encyclopedia of Human Computer Interaction*. pp. 211-219, Dec. 2005.

[53] D. Bruneau, M. A. Sasse, and J. D. McCarthy, "The eyes never lie: The use of eye tracking data in HCI research," in *Proceedings of the CHI'02 Workshop on Physiological Computing*, April 2002.

[54] M. A. Just and P. A. Carpenter, "Eye Fixations and Cognitive Processes. *Cognitive Psychology*, vol. 8, pp. 441-480, 1976.

[55] A. Darwish and E. Bataineh, "Eye Tracking Analysis of Browser Security Indicators." *Proceeding of the IEEE International Conference on Computer Systems and Industrial Informatics – ICCSII*, Dec. 2012.

[56] A. Duchowski. *Eye tracking methodology. Theory and Practice*. London: Springer-Verlag Ltd, pp.112-115, 2003.

[57] S. Bengio and J. Mareithoz, "A statistical significance test for person authentication", In *Proceedings of ODYSY- The Speaker and Language Recognition Workshop,* pp. 237-244, 2004.

[58] W. Shen, M. Surette, and R. Khanna, "Evaluation of automated biometrics-based identification and verification systems," In *Proceedings of the IEEE* , vol.85, no.9, pp.1464,1478, Sep. 1997.

[59] H. J. Goldberg and A. M. Wichansky, "Eye tracking in usability evaluation: A practitioner's guide," In *The mind's eye: Cognitive and applied aspects of eye movement research*. J. Hyönä, R. Radach, and H. Deubel Ed. Amsterdam: Elsevier, pp. 493-516, 2005.

[60] Tobii technology. "Tobii T/X series Eye Trackers." Internet: www.tobii.com/Global/ Analysis/Downloads/Product_Descriptions/Tobii_TX_Product_description.pdf.[Sep.13, 2012].

[61] Tobii Technology. "Tobii T120 Eye Tracker," Internet: http://www.tobii.com/en/eye-tracking-research/global/products/software/tobii-analytics-software-development-kit/support-downloads/, Jan. 2011 [Mar. 2012].

[62] J. F. Delvenne, A. Cleeremans, and C. Laloyaux, "Feature bindings are maintained in visual short-term memory without sustained focused attention." *Experimental Psychology*, vol. 57, issue 2, pp.108-116, 2010.

[63] J. F. Delvenne, "The capacity of visual short-term memory within and between hemifields." *Cognition*, vol. 96, pp.79-88, 2005.

[64] A. Hollingworth, "Constructing visual representations of natural scenes: The roles of short- and long-term visual memory." *Journal of Experimental Psychology: Human Perception & Performance*, vol. 30, pp.519-537, 2004.

[65] B. Ngugi, B. K. Kahn, and M. Tremaine, "Typing Biometrics: Impact of Human Learning on Performance Quality." *Journal of Data and Information Quality,* vol. 2, issue 2, pp. 1- 21, Feb. 2011.

[66] W. Neuhuber and F. Schrödl, "Autonomic control of the eye and the iris." *Autonomic Neuroscience*, vol 165, Issue 1, pp. 67-79, Nov. 2011.

[67] A. Oppenheim. *Signals and systems*, 2nd ed. London: Prentice-Hall, 1997.

[68] O. V. Komogortsev, Gobert, V. Denise, V. Jayarathna, K. Sampath, D. Hyong, S. M. Gowda, "Standardization of Automated Analyses of Oculomotor Fixation and Saccadic Behaviors." *IEEE Transactions on Biomedical Engineering*, vol. 57, no. 11, pp. 2635 – 2645, Nov. 2010.

[69] A. Olsen, "The Tobii I-VT Fixation Filter- Algorithm Description" http://www.tobii.com/en/eye-tracking-research/global/library/white-papers/the-tobii-i-vt-fixation-filter/, March 20, 2012 [Jan 10, 2013].

[70] T. Sen, and T. Megaw, “The effects of task variables and prolonged performance on saccadic eye movement parameters.” in *Theoretical and Applied Aspects of Eye Movement Research*, A. G. Gale and F. Johnson, Ed. Amsterdam: Elsevier, pp. 103-111, 1984.

[71] P. Hancock, A. Burton, and V. Bruce, “Face Processing: Human Perception and Principal Components Analysis,” *Memory and Cognition*, vol. 24, pp. 26–40, 1996.

[72] O. Alter, P. Brown, and D. Botstein, “Singular Value Decomposition for Genome-Wide Expression Data Processing and Modeling,” in *Proceedings of the National Academy of Sciences*, pp. 101-106, 2000.

[73] I. Jolliffe, Principal Component Analysis. New York: Springer Verlag, 1986.

[74] F. Sebastiani. “Machine learning in automated text categorization.” *ACM Computing Surveys*, vol. 34, issue 1, pp. 1-47, 2002.

[75] V. M. Vergara , S. Xia, and T. P. Caudell, "Information fusion across expert groups with dependent and independent components", *Proceedings of. SPIE 7345, Multisensor, Multisource Information Fusion: Architectures, Algorithms, and Applications*, April 2009.

[76] R. Zewail, A. Elsafi, M. Saeb, N. Hamdy, "Soft and hard biometrics fusion for improved identity verification," The 2004 47th Midwest Symposium on Circuits and Systems, vol.1, no., pp. I- 225-8, July 2004.

[77] E. Lupu, and S. Emerich, ” An Approach On Bimodal Biometric Systems” *Acta Technica Napocensis Electronics and Telecommunication*. vol. 51, pp.12-19, 2010.

[78] S. Ben-Yacoub, Y. Abdeljaoued, and E. Mayoraz, “Fusion of face and speech data for person identity verification,” IEEE Transactions Neural Networks, vol. 10, pp. 1065-1074, Sept. 1999.

[79] I. Guyon, J. Weston, S. Barnhill, and V. Vapnik, “Gene selection for cancer classification using support vector machines.” *Machine Learning*, vol. 46, pp. 389-422, 2002.

[80] I. H. Witten and E. Frank. *Data Mining: Practical machine learning tools with Java implementations*. 3rd edition, San Francisco: Morgan Kaufmann, 2011.

[81] L. Breiman, Random forests. Machine learning, vol. 45, issue. 1, pp. 5–32, 2001.

[82] B. Larivière and D. Van Den Poel, “Predicting customer retention and profitability by using random forests and regression forests techniques,” *Expert Systems with Applications*, vol. 29, issue 2, pp. 472-484, 2005.

[83] J. R. Quinlan. *C4.5: Programs for Machine Learning*. San Mateo: Morgan Kaufmann, 1993.

[84] T. Kinnunen and H. Li, “*An overview of text-independent speaker recognition: From features to supervectors”* Journal of Speech Communication, vol. 52, issue 1, pp. 12-40, Jan. 2010.

[85] V. Vapnik. *Statistical Learning Theory*. New York: John Wiley and Sons, pp. 81-112, 1998.

[86] J. C. Platt. Fast training of support vector machines using sequential minimal optimization. In *Advances in kernel methods*, Bernhard 246; L. Christopher, J. C. Burges, and A. J. Smola (Eds.). MIT Press, Cambridge, MA, USA, pp. 185-208, 1999.

[87] D. Batra,G. Singhal, S. Chaudhury, "Gabor filter based fingerprint classification using support vector machines," *Proceedings of the First IEEE India Annual Conference,* pp. 256-261, Dec. 2004.

[88] M. S. Deshpande and R.S. Holambe, "Text-Independent Speaker Identification Using Hidden Markov Models," *First International Conference on Emerging Trends in Engineering and Technology,* pp. 641-644, July 2008.

[89] K. Yu, J. Mason, and J. Oglesby, "Speaker recognition using hidden Markov models, dynamic time warping and vector quantisation," In *Proceedings of the IEEE transaction on Vision, Image and Signal Processing,*vol.142, no.5, pp.313-318, Oct. 1995.

[90] N. Z. Tishby, "On the application of mixture AR hidden Markov models to text independent speaker recognition," *IEEE Transaction on Signal Processing*, vol. 39, pp. 563–570, Mar. 1991.

Vita

Ali Alhaj Darwish received his bachelor's degree in software engineering with honor from the State Engineering University of Armenia, Armenia, in 2006. He received the MSc degree in computer engineering from the American University of Sharjah, UAE in 2013. His research interests are in wireless networks, network protocols, artificial intelligence, biometrics, and computer security. He is a student member of the IEEE and ACM.